On Tchebycheff Decomposition Approaches for Multi-objective Evolutionary Optimization

Xiaoliang Ma, Qingfu Zhang, *Fellow, IEEE*, Guangdong Tian, Junshan Yang, and Zexuan Zhu, *Member, IEEE*

***Abstract*—Tchebycheff decomposition represents one of the most widely used decomposition approaches that can convert a multi-objective optimization problem into a set of scalar optimization subproblems. Nevertheless, the geometric properties of the subproblem objective functions in Tchebycheff decomposition have not been explicitly studied. This paper proposes a Tchebycheff decomposition with l_p-norm constraint on direction vectors in which the subproblem objective functions are endowed with clear geometric property. Especially, the Tchebycheff decomposition with l_2-norm constraint on direction vectors is taken as an example to illustrate its advantage. A new unary R_2 indicator is also introduced to approximate the hyper-volume metric and justify the efficiency of the proposed Tchebycheff decomposition. A resultant Tchebycheff decomposition based multi-objective evolutionary algorithm with l_2-norm constraint and a new population update strategy is proposed to solve multi-objective optimization problems. The experimental results on both benchmark and real-world multi-objective optimization problems show that the proposed algorithm is capable of obtaining high quality solutions compared with other state-of-the-art multi-objective evolutionary algorithms.**

***Index Terms*—Tchebycheff decomposition, multi-objective evolutionary algorithm based on decomposition, population update strategy, maximal fitness improvement, R_2 metric.**

I. Introduction

A Multi-objective problem (MOP) [1, 2] can be formulated as follows:

$$\begin{cases} \min \mathbf{F}(\mathbf{x}) = (f_1(\mathbf{x}), \cdots, f_m(\mathbf{x})) \\ \text{subject to} : \mathbf{x} \in \Omega \end{cases} \quad (1)$$

where $\mathbf{x}$ is a vector of decision variables, Ω is the decision space, and $\mathbf{F}(\mathbf{x}) : \Omega \rightarrow \mathbf{R}^m$ is an m-dimensional vector of m objective functions.

This work was supported in part by the National Natural Science Foundation of China, under Grants (61471246, 61603259, 51405075, and 61473241), ANR/RCC Joint Research Scheme sponsored by the Research Grants Council of the Hong Kong Special Administrative Region, China and France National Research Agency, under Grant A-CityU101/16, Guangdong Special Support Program of Top-notch Young Professionals, under Grant 2014TQ01X273, Fundamental Research Funds for the Central Universities, under Grants (GK201603014 and GK201603082), and China Postdoctoral Science Foundation, under Grant 2016M592536.(Corresponding author: Zexuan Zhu.)

X. Ma and Z. Zhu are with the Shenzhen City Key Laboratory of Embedded System Design, College of Computer Science and Software Engineering, Shenzhen University, Shenzhen 518060, China (e-mail: maxiaoliang@yeah.net; zhuzx@szu.edu.cn).

Q. Zhang is with the Department of Computer Science, City University of Hong Kong, Hong Kong, and Shenzhen Research Institute, City University of Hong Kong, Shenzhen, China.(email: qingfu.zhang@cityu.edu.hk)

G. Tian is with the College of Transportation, Jilin University, China.(e-mail: tiangd2013@gmail.com)

J. Yang is with College of Information Engineering, Shenzhen University, Shenzhen 518060, China.(e-mail: junshan763@126.com)

Manuscript received December, 2015.

Let $\mathbf{x}_a$ and $\mathbf{x}_b$ be two decision vectors. $\mathbf{x}_a$ is said to dominate $\mathbf{x}_b$ (denoted by $\mathbf{x}_a \prec \mathbf{x}_b$), if and only if $\forall i \in \{1, \cdots, m\}, f_i(\mathbf{x}_a) \leq f_i(\mathbf{x}_b)$ and $\mathbf{F}(\mathbf{x_a}) \neq \mathbf{F}(\mathbf{x_b})$. A solution $\mathbf{x}^* \in \Omega$ is called Pareto optimal if it is not dominated by any other solution. All Pareto optimal solutions form the Pareto optimal set (PS), i.e., $PS = \{\mathbf{x}^* \mid \nexists \mathbf{x} \in \Omega, \mathbf{x} \prec \mathbf{x}^*\}$. The corresponding set of optimal objective vectors is called the Pareto optimal front (PF), i.e., $PF = \{\mathbf{F}(\mathbf{x}) \mid \mathbf{x} \in PS\}$.

Multi-objective evolutionary algorithm based on decomposition (MOEA/D) has been identified as one of the most effective methods [3–14] to approximate the PF. The decomposition approach is a key component of MOEA/D. Tchebycheff decomposition is one of the most widely used decomposition approaches. However, the solutions obtained by Tchebycheff decomposition with uniform weight vectors are not always uniformly distributed [5–9]. The generalized decomposition [5–7] and modified Tchebycheff decomposition [9, 10] have been proposed to deal with this issue, yet the geometric properties of the subproblem objective functions in these Tchebycheff decomposition methods have not been explicitly studied.

This paper proposes a Tchebycheff decomposition approach with l_p-norm constraint on direction vectors (p-Tch) in which the subproblem objective functions have clear geometric property. The relationships between the p-Tch and other Tchebycheff decomposition approaches are investigated. Different p values impose different competition pressures among the subproblems in MOEA/D. The Tchebycheff decomposition with l_2-norm constraint (2-Tch) is taken as an example to illustrate the advantages of the proposed decomposition approach. Indicator R_2^{2tch}, a variant of R_2 indicator [15] based on 2-Tch, is also introduced to approximate the hyper-volume metric to justify the efficiency of the proposed Tchebycheff decomposition.

The 2-Tch is used in MOEA/D framework with a new population update strategy. In most of the MOEA/D variants (e.g., [4, 16–18]), the evolution population is updated based on a local stochastic strategy. It is in [19] that a global strategy based on minimal fitness value was proposed. However, the aforementioned strategies are all designed to optimize the performance of some individual subproblem(s) rather than all subproblems. To deal with this issue, this paper introduces a global population update strategy based on maximal fitness improvement to optimize the general performance of all subproblems. The resultant algorithm, MOEA/D-2TCHMFI (MOEA/D based on 2-Tch and population update strategy with maximal fitness improvement), is tested on various benchmark and real-world MOPs. The experimental results show that

MOEA/D-2TCHMFI is capable of obtaining high quality solutions compared with other state-of-the-art multi-objective evolutionary algorithms.

In the rest of this paper, Section II reviews two closely related Tchebycheff decomposition approaches. The proposed Tchebycheff decomposition with l_p-norm constraint on direction vectors and a generalized form of decomposition are introduced in Section III. Section IV presents the population update strategy based on maximal fitness improvement. The resultant MOEA/D-2TCHMFI algorithm is described in Section V. Section VI defines the proposed unary indicator R_2^{2tch}. Section VII shows the comparison results between MOEA/D-2TCHMFI and other state-of-the-art multi-objective evolutionary algorithms. Finally, Section VIII concludes this work.

II. Two closely related Tchebycheff decomposition methods

In this section, we review two closely related Tchebycheff decomposition approaches, i.e., the conventional Tchebycheff decomposition [20] and the modified Tchebycheff decomposition [10]. The geometric property of the subproblem objective functions in these two Tchebycheff decomposition approaches is investigated in detail.

A. Conventional Tchebycheff decomposition

The conventional Tchebycheff decomposition decomposes an MOP into a set of scalar optimization subproblems, each of which is defined as follows:

$$\min_{\mathbf{x}\in\Omega} g^{tch}(\mathbf{F}(\mathbf{x})|\mathbf{w},\mathbf{z}^*) = \max_{1\le i\le m}\{w_i(f_i(\mathbf{x})-z_i^*)\} \tag{2}$$

where $\mathbf{w}=(w_1,\ldots,w_m)$ with $\sum_{i=1}^m w_i = 1$ and $w_i \ge 0$ is the weight vector of a subproblem, and $\mathbf{z}^*=(z_1^*,\ldots,z_m^*)$ with $z_i^* < \min\{f_i(\mathbf{x})|\mathbf{x}\in\Omega\}$ is an ideal objective vector.

The geometric property of the subproblem objective functions has not been studied in the conventional Tchebycheff decomposition. To the best of our knowledge, this work represents the first attempt to study the geometric property of the subproblem objective functions in Tchebycheff decomposition.

Proposition 2.1: Let $\mathbf{z}^*=(z_1^*,\ldots,z_m^*)$ be an ideal objective vector of (1) and $\mathbf{w}=(w_1,\ldots,w_m)$ be a positive weight vector. If a given objective vector $\mathbf{F}(\mathbf{x})=(f_1(\mathbf{x}),\ldots,f_m(\mathbf{x}))$ is in the line

$$\mathbf{L}_1 : w_1(f_1(\mathbf{x})-z_1^*) = \cdots = w_m(f_m(\mathbf{x})-z_m^*)$$

as shown in Fig. 1 (a). Then

$$g^{tch}(\mathbf{F}(\mathbf{x})|\mathbf{w},\mathbf{z}^*) = \frac{\mathbf{w}^T(\mathbf{F}(\mathbf{x})-\mathbf{z}^*)}{m} \tag{3}$$

Proof. Since $\mathbf{F}(\mathbf{x})$ is in the line $\mathbf{L}_1$, we obtain

$$\begin{aligned} g^{tch}(\mathbf{F}(\mathbf{x})|\mathbf{w},\mathbf{z}^*) &\overset{(2)}{=\!=} \max_{1\le i\le m}\{w_i(f_i(\mathbf{x})-z_i^*)\} \\ &\overset{\mathbf{L}_1}{=\!=} w_1(f_1(\mathbf{x})-z_1^*) = \cdots = w_m(f_m(\mathbf{x})-z_m^*) \\ &= \frac{\sum_{i=1}^m w_i(f_i(\mathbf{x})-z_i^*)}{m} = \frac{\mathbf{w}^T(\mathbf{F}(\mathbf{x})-\mathbf{z}^*)}{m} \end{aligned}$$ ■

Equation (3) is used to illustrate the geometric property of $g^{tch}(\mathbf{F}(\mathbf{x})|\mathbf{w},\mathbf{z}^*)$ instead of finding the optimal solution of $g^{tch}(\mathbf{F}(\mathbf{x})|\mathbf{w},\mathbf{z}^*)$, i.e., $\min_{\mathbf{x}\in\Omega} g^{tch}(\mathbf{F}(\mathbf{x})|\mathbf{w},\mathbf{z}^*)$. Taking $\mathbf{F}(\mathbf{x})=(1/2,1/4)$, $\mathbf{z}^*=(0,0)$, and $\mathbf{w}=(1/3,2/3)$ for example as shown in Fig. 1 (a), we can use equation (3) to explain the relationship between the subproblem fitness value $g^{tch}(\mathbf{F}(\mathbf{x})|\mathbf{w},\mathbf{z}^*)$, $\mathbf{w}$, and $\mathbf{F}(\mathbf{x})-\mathbf{z}^*$. Equation (3) (i.e., $\mathbf{w}^T(\mathbf{F}(\mathbf{x})-\mathbf{z}^*)/m$) gives a weighted form of l_1-norm, which is a dual expression of $g^{tch}(\mathbf{F}(\mathbf{x})|\mathbf{w},\mathbf{z}^*)$ [21, pp. 637].

A case where $\mathbf{F}(\mathbf{x})$ does not lie in $\mathbf{L}_1$ is described in the following proposition.

Proposition 2.2: Let $\mathbf{z}^*=(z_1^*,\ldots,z_m^*)$ be an ideal objective vector of (1) and $\mathbf{w}=(w_1,\ldots,w_m)$ be a positive weight vector. Given an objective vector $\mathbf{F}(\mathbf{x})=(f_1(\mathbf{x}),\ldots,f_m(\mathbf{x}))$, $\hat{\mathbf{F}}(\mathbf{x})=(\hat{f}_1(\mathbf{x}),\ldots,\hat{f}_m(\mathbf{x}))$ is constructed such that: **1)** $\hat{\mathbf{F}}(\mathbf{x})$ and $\mathbf{F}(\mathbf{x})$ have the same subproblem fitness value, i.e., $g^{tch}(\mathbf{F}(\mathbf{x})|\mathbf{w},\mathbf{z}^*) = g^{tch}(\hat{\mathbf{F}}(\mathbf{x})|\mathbf{w},\mathbf{z}^*)$; **2)** $\hat{\mathbf{F}}(\mathbf{x})$ is in the line $\mathbf{L}_1$ as shown in Fig. 1 (d). Then, the following equation holds:

$$g^{tch}(\mathbf{F}(\mathbf{x})|\mathbf{w},\mathbf{z}^*) = \frac{\mathbf{w}^T(\hat{\mathbf{F}}(\mathbf{x})-\mathbf{z}^*)}{m} \tag{4}$$

Proof. From the construction of $\hat{\mathbf{F}}(\mathbf{x})$, we get

$$g^{tch}(\mathbf{F}(\mathbf{x})|\mathbf{w},\mathbf{z}^*) \overset{1)}{=\!=} g^{tch}(\hat{\mathbf{F}}(\mathbf{x})|\mathbf{w},\mathbf{z}^*) \overset{\substack{2)\ \hat{\mathbf{F}}(\mathbf{x})\text{ is in }\mathbf{L}_1 \\ Proposition\ 2.1}}{=\!=} \frac{\mathbf{w}^T(\hat{\mathbf{F}}(\mathbf{x})-\mathbf{z}^*)}{m}$$ ■

Remark. Given an objective vector $\mathbf{F}(\mathbf{x})$, $\hat{\mathbf{F}}(\mathbf{x}) = (\hat{f}_1(\mathbf{x}),\ldots,\hat{f}_m(\mathbf{x}))$ is actually the intersection point between $\mathbf{L}_1$ and the contour line of $g^{tch}(\mathbf{F}(\mathbf{x})|\mathbf{w},\mathbf{z}^*)$ in the objective space, as shown in Fig. 1 (d), and

$$\hat{f}_i(\mathbf{x}) = z_i^* + \frac{g^{tch}(\mathbf{F}(\mathbf{x})|\mathbf{w},\mathbf{z}^*)}{w_i}, i=1,\ldots,m$$

due to the fact:

$$\begin{aligned} g^{tch}(\mathbf{F}(\mathbf{x})|\mathbf{w},\mathbf{z}^*) &\overset{1)}{=\!=} g^{tch}(\hat{\mathbf{F}}(\mathbf{x})|\mathbf{w},\mathbf{z}^*) \\ &\overset{2)}{=\!=} w_1(\hat{f}_1(\mathbf{x})-z_1^*) = \cdots = w_m(\hat{f}_m(\mathbf{x})-z_m^*) \end{aligned}$$ ■

Taking $\mathbf{F}(\mathbf{x})=(1,1)$, $\mathbf{z}^*=(0,0)$, and $\mathbf{w}=(1/3,2/3)$ for example, we can obtain:

$$\begin{aligned} g^{tch}(\mathbf{F}(\mathbf{x})|\mathbf{w},\mathbf{z}^*) &= \max\left\{\frac{1}{3}(1-0),\frac{2}{3}(1-0)\right\} = 2/3, \\ \hat{f}_1(\mathbf{x}) &= z_1^* + \frac{g^{tch}(\mathbf{F}(\mathbf{x})|\mathbf{w},\mathbf{z}^*)}{w_1} = 0 + \frac{2/3}{1/3} = 2, \\ \hat{f}_2(\mathbf{x}) &= z_2^* + \frac{g^{tch}(\mathbf{F}(\mathbf{x})|\mathbf{w},\mathbf{z}^*)}{w_2} = 0 + \frac{2/3}{2/3} = 1. \end{aligned}$$

B. Modified Tchebycheff decomposition

To handle the nonlinear relationship [5–8, 22–24] between the optimal solutions and the corresponding subproblem weight vectors, the work [10] proposed a modified Tchebycheff decomposition. Instead of multiplying w_i in (2), the modified Tchebycheff decomposition constructs subproblems by dividing $f_i(\mathbf{x})-z_i^*$ by w_i as follows:

$$\min_{\mathbf{x}\in\Omega} g^{mtch}(\mathbf{F}(\mathbf{x})|\mathbf{w},\mathbf{z}^*) = \max_{1\le i\le m}\left\{\frac{f_i(\mathbf{x})-z_i^*}{w_i}\right\} \tag{5}$$

The geometric property of a subproblem objective function in the modified Tchebycheff decomposition is studied as follows.

Proposition 2.3: Let $\mathbf{z}^* = (z_1^*, \ldots, z_m^*)$ be an ideal objective vector of (1) and $\mathbf{w} = (w_1, \ldots, w_m)$ be a positive weight vector. If a given objective vector $\mathbf{F}(\mathbf{x}) = (f_1(\mathbf{x}), \ldots, f_m(\mathbf{x}))$ is in the line

$$\mathbf{L}_2 : \frac{f_1(\mathbf{x}) - z_1^*}{w_1} = \cdots = \frac{f_m(\mathbf{x}) - z_m^*}{w_m}$$

as shown in Fig.1 (b). Then,

$$g^{mtch}(\mathbf{F}(\mathbf{x})|\mathbf{w}, \mathbf{z}^*) = \|\mathbf{F}(\mathbf{x}) - \mathbf{z}^*\|_1 \tag{6}$$

Proof. Since $\mathbf{F}(\mathbf{x})$ is in $\mathbf{L}_2$, we can infer that

$$\begin{aligned} g^{mtch}(\mathbf{F}(\mathbf{x})|\mathbf{w}, \mathbf{z}^*) &\overset{(5)}{=\!=} \max_{1\le i\le m}\left\{\frac{f_i(\mathbf{x}) - z_i^*}{w_i}\right\} \\ &\overset{\mathbf{L}_2}{=\!=} \frac{f_1(\mathbf{x}) - z_1^*}{w_1} = \cdots = \frac{f_m(\mathbf{x}) - z_m^*}{w_m} \\ &= \frac{\sum_{i=1}^m (f_i(\mathbf{x}) - z_i^*)}{\sum_{i=1}^m w_i} = \|\mathbf{F}(\mathbf{x}) - \mathbf{z}^*\|_1 \end{aligned}$$

■

Taking $\mathbf{F}(\mathbf{x}) = (1/4, 2/4)$, $\mathbf{z}^* = (0, 0)$, and $\mathbf{w} = (1/3, 2/3)$ for example, equation (6) is calculated as follows:

$$\begin{aligned} g^{mtch}(\mathbf{F}(\mathbf{x})|\mathbf{w}, \mathbf{z}^*) &= \max\left\{\frac{f_1(\mathbf{x}) - z_1^*}{w_1}, \frac{f_2(\mathbf{x}) - z_2^*}{w_2}\right\} \\ &= \max\left\{\frac{1/4 - 0}{1/3}, \frac{2/4 - 0}{2/3}\right\} = \frac{3}{4} = \|\mathbf{F}(\mathbf{x}) - \mathbf{z}^*\|_1 \end{aligned}$$

In situations where $\mathbf{F}(\mathbf{x})$ is not in $\mathbf{L}_2$, the following proposition depicts the geometric property of $g^{tch}(\mathbf{F}(\mathbf{x})|\mathbf{w}, \mathbf{z}^*)$.

Proposition 2.4: Let $\mathbf{z}^* = (z_1^*, \ldots, z_m^*)$ be an ideal objective vector of (1) and $\mathbf{w} = (w_1, \ldots, w_m)$ be a positive weight vector. Given an objective vector $\mathbf{F}(\mathbf{x}) = (f_1(\mathbf{x}), \ldots, f_m(\mathbf{x}))$, $\tilde{\mathbf{F}}(\mathbf{x}) = (\tilde{f}_1(\mathbf{x}), \ldots, \tilde{f}_m(\mathbf{x}))$ is generated to satisfy two constraints: **1**) $\tilde{\mathbf{F}}(\mathbf{x})$ and $\mathbf{F}(\mathbf{x})$ are located in the same contour line, i.e., $g^{mtch}(\mathbf{F}(\mathbf{x})|\mathbf{w}, \mathbf{z}^*) = g^{mtch}(\tilde{\mathbf{F}}(\mathbf{x})|\mathbf{w}, \mathbf{z}^*)$; and **2**) $\tilde{\mathbf{F}}(\mathbf{x})$ lies in the line $\mathbf{L}_2$ as shown in Fig. 1 (e). Then,

$$g^{mtch}(\mathbf{F}(\mathbf{x})|\mathbf{w}, \mathbf{z}^*) = \|\tilde{\mathbf{F}}(\mathbf{x}) - \mathbf{z}^*\|_1 \tag{7}$$

Proof. According to the conditions of $\tilde{\mathbf{F}}(\mathbf{x})$, we get

$$\begin{aligned} g^{mtch}(\mathbf{F}(\mathbf{x})|\mathbf{w}, \mathbf{z}^*) &\overset{1)}{=\!=} g^{mtch}(\tilde{\mathbf{F}}(\mathbf{x})|\mathbf{w}, \mathbf{z}^*) \\ &\overset{\substack{2)\ \tilde{\mathbf{F}}(\mathbf{x})\ \text{is in}\ \mathbf{L}_2 \\ Proposition\ 2.3}}{=\!=\!=} \|\tilde{\mathbf{F}}(\mathbf{x}) - \mathbf{z}^*\|_1 \end{aligned}$$

■

Remark. In geometry, $g^{mtch}(\mathbf{F}(\mathbf{x})|\mathbf{w}, \mathbf{z}^*)$ is equal to the l_1-norm of $\tilde{\mathbf{F}}(\mathbf{x}) - \mathbf{z}^*$ as shown in Fig. 1 (e). $\tilde{\mathbf{F}}(\mathbf{x})$ is the intersection point between line $\mathbf{L}_2$ and the contour line of $g^{mtch}(\mathbf{F}(\mathbf{x})|\mathbf{w}, \mathbf{z}^*)$ in the objective space as shown in Fig. 1 (e).

$$\tilde{\mathbf{F}}(\mathbf{x}) = (\tilde{f}_1(\mathbf{x}), \ldots, \tilde{f}_m(\mathbf{x})) = \mathbf{z}^* + g^{mtch}(\mathbf{F}(\mathbf{x})|\mathbf{w}, \mathbf{z}^*) \cdot \mathbf{w}$$

since

$$\begin{aligned} g^{mtch}(\mathbf{F}(\mathbf{x})|\mathbf{w}, \mathbf{z}^*) &\overset{1)}{=\!=} g^{mtch}(\tilde{\mathbf{F}}(\mathbf{x})|\mathbf{w}, \mathbf{z}^*) \\ &\overset{\substack{2) \\ \mathbf{L}_2}}{=\!=} \frac{\tilde{f}_1(\mathbf{x}) - z_1^*}{w_1} = \cdots = \frac{\tilde{f}_m(\mathbf{x}) - z_m^*}{w_m} \end{aligned}$$

■

For example, given $\mathbf{F}(\mathbf{x}) = (0.5, 2)$, $\mathbf{z}^* = (0, 0)$, and $\mathbf{w} = (1/3, 2/3)$, we can calculate

$$\begin{aligned} &g^{mtch}(\mathbf{F}(\mathbf{x})|\mathbf{w}, \mathbf{z}^*) = \max\left\{\frac{0.5 - 0}{1/3}, \frac{2 - 0}{2/3}\right\} = 3, \\ &\tilde{f}_1(\mathbf{x}) = z_1^* + g^{mtch}(\mathbf{F}(\mathbf{x})|\mathbf{w}, \mathbf{z}^*) \cdot w_1 = 0 + 3 \cdot 1/3 = 1, \\ &\tilde{f}_2(\mathbf{x}) = z_2^* + g^{mtch}(\mathbf{F}(\mathbf{x})|\mathbf{w}, \mathbf{z}^*) \cdot w_2 = 0 + 3 \cdot 2/3 = 2. \end{aligned}$$

III. The Proposed Tchebycheff Decomposition with l_p-norm Constraint on Direction Vectors

By extending the modified Tchebycheff decomposition, this paper proposes a novel Tchebycheff decomposition approach with l_p-norm constraint on direction vectors, called p-Tch for short. In p-Tch, each subproblem is constructed based on a direction vector $\boldsymbol{\lambda}$ with $\|\boldsymbol{\lambda}\|_p = 1$ rather than a weight vector $\mathbf{w}$ with $\|\mathbf{w}\|_1 = \sum_{i=1}^m w_i = 1$ as used in the modified Tchebycheff decomposition, i.e.,

$$\min_{\mathbf{x}\in\Omega} g^{ptch}(\mathbf{F}(\mathbf{x})|\boldsymbol{\lambda}, \mathbf{z}^*) = \max_{1\le i\le m}\left\{\frac{f_i(\mathbf{x}) - z_i^*}{\lambda_i}\right\} \tag{8}$$

where $\boldsymbol{\lambda} = (\lambda_1, \ldots, \lambda_m)$ with $\|\boldsymbol{\lambda}\|_p = 1$ and $\lambda_1, \ldots, \lambda_m > 0$. Note that the modified Tchebycheff decomposition (5) is a special case of p-Tch with $p = 1$, and, similar to Chebyshev approximation problem [21, pp. 293], an equivalent problem of p-Tch (8) can be formulated as follows:

$$\begin{cases} \min\limits_{\mathbf{x}\in\Omega} & t \\ \text{s.t.} & \frac{f_i(\mathbf{x}) - z_i^*}{\lambda_i} \le t, i = 1, ..., m \end{cases}$$

A. Geometric property of a subproblem objective function in the p-Tch

Proposition 3.1: Let $\mathbf{z}^* = (z_1^*, \ldots, z_m^*)$ be an ideal objective vector of (1) and the direction vector $\boldsymbol{\lambda}$ be a positive vector with $\|\boldsymbol{\lambda}\|_p = 1$. If a given objective vector $\mathbf{F}(\mathbf{x}) = (f_1(\mathbf{x}), \ldots, f_m(\mathbf{x}))$ is in the line

$$\mathbf{L}_3 : \frac{f_1(\mathbf{x}) - z_1^*}{\lambda_1} = \cdots = \frac{f_m(\mathbf{x}) - z_m^*}{\lambda_m}.$$

Then

$$g^{ptch}(\mathbf{F}(\mathbf{x})|\boldsymbol{\lambda}, \mathbf{z}^*) = \|\mathbf{F}(\mathbf{x}) - \mathbf{z}^*\|_p \tag{9}$$

Proof. Since $f_i(\mathbf{x}) - z_i^* \ge 0$ and $\lambda_i > 0$ for $\forall i \in \{1, 2, ..., m\}$,

$$\begin{aligned} k(\mathbf{x}) \triangleq g^{ptch}(\mathbf{F}(\mathbf{x})|\boldsymbol{\lambda}, \mathbf{z}^*) &\overset{(8)}{=\!=} \max_{1\le i\le m}\left\{\frac{f_i(\mathbf{x}) - z_i^*}{\lambda_i}\right\} \\ &\overset{\mathbf{L}_3}{=\!=} \frac{f_1(\mathbf{x}) - z_1^*}{\lambda_1} = \cdots = \frac{f_m(\mathbf{x}) - z_m^*}{\lambda_m} \ge 0 \end{aligned} \tag{10}$$

Since $f_i(\mathbf{x}) - z_i^* = \lambda_i \cdot k(\mathbf{x})$ for $i = 1, \ldots, m$ and $\mathbf{F}(\mathbf{x}) - \mathbf{z}^* = k(\mathbf{x}) \cdot \boldsymbol{\lambda}$, we have

$$\begin{aligned} g^{ptch}(\mathbf{F}(\mathbf{x})|\boldsymbol{\lambda}, \mathbf{z}^*) = k(\mathbf{x}) &\overset{\|\boldsymbol{\lambda}\|_p = 1}{=\!=\!=} k(\mathbf{x}) \cdot \|\boldsymbol{\lambda}\|_p \overset{\substack{k(\mathbf{x})\ge 0 \\ (10)}}{=\!=\!=} \\ \|k(\mathbf{x}) \cdot \boldsymbol{\lambda}\|_p &\overset{k(\mathbf{x})\cdot\boldsymbol{\lambda} = \mathbf{F}(\mathbf{x}) - \mathbf{z}^*}{=\!=\!=\!=} \|\mathbf{F}(\mathbf{x}) - \mathbf{z}^*\|_p \end{aligned} \tag{11}$$

■

This article has been accepted for publication in a future issue of this journal, but has not been fully edited. Content may change prior to final publication. Citation information: DOI 10.1109/TEVC.2017.2704118, IEEE Transactions on Evolutionary Computation

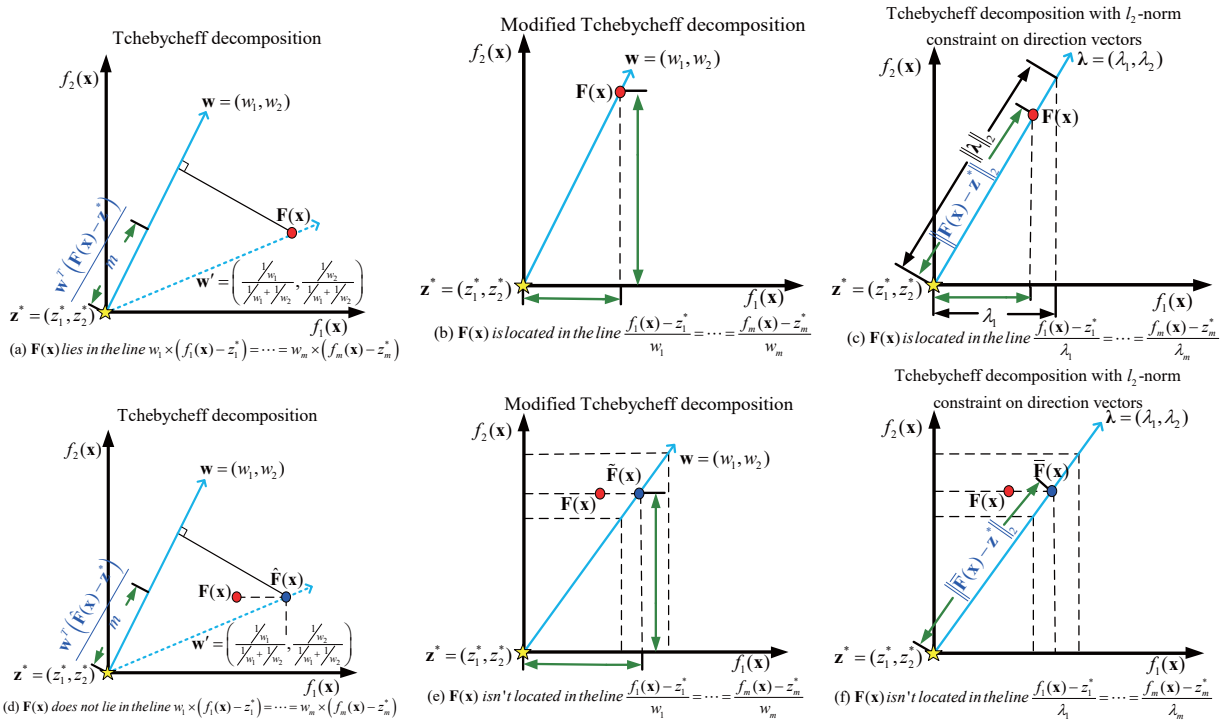

Fig. 1. The geometric property of the subproblems in the three Tchebycheff decomposition approaches.

Taking $p=2$, $\mathbf{F}(\mathbf{x})=(1,2)$, $\boldsymbol{\lambda}=(1/\sqrt{5},2/\sqrt{5})$, and $\mathbf{z}^*=(0,0)$ for example, we can obtain

$$g^{2tch}(\mathbf{F}(\mathbf{x})|\boldsymbol{\lambda},\mathbf{z}^*)=\max\left\{\frac{f_1(\mathbf{x})-z_1^*}{\lambda_1},\frac{f_2(\mathbf{x})-z_2^*}{\lambda_2}\right\}$$
$$=\max\left\{\frac{1-0}{1/\sqrt{5}},\frac{2-0}{2/\sqrt{5}}\right\}=\sqrt{5}=\|\mathbf{F}(\mathbf{x})-\mathbf{z}^*\|_2$$

The case described in *Proposition* 3.1 with $p=2$ is illustrated in Fig. 1 (c). It is shown that $g^{ptch}(\mathbf{F}(\mathbf{x})|\boldsymbol{\lambda},\mathbf{z}^*)$ is the Euclidean distance from $\mathbf{z}^*$ to $\mathbf{F}(\mathbf{x})$ when $p=2$. A case where $\mathbf{F}(\mathbf{x})$ does not lie in $\mathbf{L}_3$ is described in the following proposition.

Proposition 3.2: Let $\mathbf{z}^*=(z_1^*,\ldots,z_m^*)$ be an ideal objective vector of (1) and the direction vector $\boldsymbol{\lambda}$ be a positive vector with $\|\boldsymbol{\lambda}\|_p=1$. Given an objective vector $\mathbf{F}(\mathbf{x})=(f_1(\mathbf{x}),\ldots,f_m(\mathbf{x}))$, $\bar{\mathbf{F}}(\mathbf{x})=(\bar{f}_1(\mathbf{x}),\ldots,\bar{f}_m(\mathbf{x}))$ satisfies two constraints: **1)** $\bar{\mathbf{F}}(\mathbf{x})$ and $\mathbf{F}(\mathbf{x})$ have the same fitness, i.e., $g^{ptch}(\mathbf{F}(\mathbf{x})|\boldsymbol{\lambda},\mathbf{z}^*)=g^{ptch}(\bar{\mathbf{F}}(\mathbf{x})|\boldsymbol{\lambda},\mathbf{z}^*)$; **2)** $\bar{\mathbf{F}}(\mathbf{x})$ lies in the straight line $\mathbf{L}_3$ as shown in Fig. 1 (f). Then,

$$g^{ptch}(\mathbf{F}(\mathbf{x})|\boldsymbol{\lambda},\mathbf{z}^*)=\|\bar{\mathbf{F}}(\mathbf{x})-\mathbf{z}^*\|_p \tag{12}$$

Proof. From the construction of $\bar{\mathbf{F}}(\mathbf{x})$, we can get

$$g^{ptch}(\mathbf{F}(\mathbf{x})|\boldsymbol{\lambda},\mathbf{z}^*)\overset{1)}{=\!=}g^{ptch}(\bar{\mathbf{F}}(\mathbf{x})|\boldsymbol{\lambda},\mathbf{z}^*)$$
$$\overset{\substack{2)\ \bar{\mathbf{F}}(\mathbf{x})\ \text{is in}\ \mathbf{L}_3\\ Proposition\ 3.1}}{=\!=\!=}\|\bar{\mathbf{F}}(\mathbf{x})-\mathbf{z}^*\|_p \qquad \blacksquare$$

According to the two constraints of $\bar{\mathbf{F}}(\mathbf{x})$, we can obtain

$$\bar{\mathbf{F}}(\mathbf{x})=(\bar{f}_1(\mathbf{x}),\ldots,\bar{f}_m(\mathbf{x}))=\mathbf{z}^*+g^{ptch}(\mathbf{F}(\mathbf{x})|\boldsymbol{\lambda},\mathbf{z}^*)\cdot\boldsymbol{\lambda}$$

For example, given $p=2$, $\mathbf{F}(\mathbf{x})=(0.5,2)$, $\boldsymbol{\lambda}=(1/\sqrt{5},2/\sqrt{5})$, and $\mathbf{z}^*=(0,0)$, we can calculate that

$$g^{2tch}(\mathbf{F}(\mathbf{x})|\boldsymbol{\lambda},\mathbf{z}^*)=\max\left\{\frac{0.5-0}{1/\sqrt{5}},\frac{2-0}{2/\sqrt{5}}\right\}=\sqrt{5},$$
$$\bar{f}_1(\mathbf{x})=z_1^*+g^{2tch}(\mathbf{F}(\mathbf{x})|\boldsymbol{\lambda},\mathbf{z}^*)\cdot\lambda_1=0+\sqrt{5}\cdot 1/\sqrt{5}=1,$$
$$\bar{f}_2(\mathbf{x})=z_2^*+g^{2tch}(\mathbf{F}(\mathbf{x})|\boldsymbol{\lambda},\mathbf{z}^*)\cdot\lambda_2=0+\sqrt{5}\cdot 2/\sqrt{5}=2.$$

B. Relationship between the modified Tchebycheff decomposition and the p-Tch

The modified Tchebycheff decomposition and the p-Tch share similarity in constructing subproblems, i.e.,

$$g^{ptch}(\mathbf{F}(\mathbf{x})|\boldsymbol{\lambda},\mathbf{z}^*)\overset{\boldsymbol{\lambda}=\frac{\mathbf{w}}{\|\mathbf{w}\|_p}}{=\!=\!=\!=}g^{ptch}(\mathbf{F}(\mathbf{x})|\frac{\mathbf{w}}{\|\mathbf{w}\|_p},\mathbf{z}^*)$$
$$\overset{(8)}{=\!=}\max_{1\le i\le m}\left\{\frac{f_i(\mathbf{x})-z_i^*}{\frac{w_i}{\|\mathbf{w}\|_p}}\right\}=\|\mathbf{w}\|_p\cdot\max_{1\le i\le m}\left\{\frac{f_i(\mathbf{x})-z_i^*}{w_i}\right\}$$
$$\overset{(5)}{=\!=}\|\mathbf{w}\|_p\cdot g^{mtch}(\mathbf{F}(\mathbf{x})|\mathbf{w},\mathbf{z}^*) \tag{13}$$

where the p-Tch differs from the modified Tchebycheff decomposition by introducing a weight factor $\|\mathbf{w}\|_p$.

Equation (13) can be generalized. More specifically, if $g(\mathbf{F}(\mathbf{x})|\mathbf{w},\mathbf{z}^*)$ denotes a subproblem of a decomposition method, e.g., the conventional Tchebycheff decomposition, the modified Tchebycheff decomposition, the weight sum method [20], or the PBI method [3], then a generalized subproblem objective function can be defined as $c(\mathbf{w})\cdot g(\mathbf{F}(\mathbf{x})|\mathbf{w},\mathbf{z}^*)$, where $c(\mathbf{w})$ is a coefficient merely depending on the weight vector $\mathbf{w}$ and $c(\mathbf{w})>0$ holds for any $\mathbf{w}$. In p-Tch, $c(\mathbf{w})=\|\mathbf{w}\|_p$.

TABLE I
PERCENTAGE OF THE GENERALIZED SUBPROBLEM PREFERENCE REGION WITH DIFFERENT VALUES OF $c(\mathbf{w})$.

Percentage of subproblem preference region	Subproblem with $\mathbf{w}^1$	Subproblem with $\mathbf{w}^2$	Subproblem with $\mathbf{w}^3$
$c(\mathbf{w}) = \|\mathbf{w}\|_{0.1}^4$	48.3%	3.4%	48.3%
$c(\mathbf{w}) = \|\mathbf{w}\|_{0.5}^4$	33.24%	33.52%	33.24%
$c(\mathbf{w}) = \|\mathbf{w}\|_{1.5}^4$	13.78%	72.44%	13.78%

C. Advantage of the proposed generalized subproblem

A main advantage of the generalized subproblem over the original subproblem is that the generalized one can adjust the importance/weight of a subproblem in competition for the chance of being updated by offspring solutions.

1) Tuning the subproblem importance by partitioning the feasible objective space: $c(\mathbf{w})$ can be regarded as the weight/importance of a subproblem. The definition of subproblem preference region is introduced as follows:

$$\Upsilon^i = \{\mathbf{F}(\mathbf{x}) | \mathbf{x} \in \Omega, \arg\min_{1 \le j \le N} \{c(\mathbf{w}^j) \cdot g(\mathbf{F}(\mathbf{x})|\mathbf{w}^j, \mathbf{z}^*)\} = i\} \tag{14}$$

where N is the number of subproblems. In Υ^i, $c(\mathbf{w}^i) \cdot g(\mathbf{F}(\mathbf{x})|\mathbf{w}^i, \mathbf{z}^*)$ is the smallest among all the $c(\mathbf{w}^j) \cdot g(\mathbf{F}(\mathbf{x})|\mathbf{w}^j, \mathbf{z}^*), j = 1, \ldots, N$. Other ways to define subproblem preference regions can be found in [25, 26].

The effect of $c(\mathbf{w})$ on the partition of the feasible objective space using the modified Tchebycheff decomposition is shown in Fig. 2 and Table I based on (14). In Fig. 2, $c(\mathbf{w}) = \|\mathbf{w}\|_p^4$ is used and p is set to 0.1, 0.5, and 1.5 in the three subfigures, respectively. It is shown that increasing p value decreases the preference regions of the boundary subproblems, i.e., the subproblems associated with $\mathbf{w}^1$ and $\mathbf{w}^3$, and increases the preference region of the intermediary subproblem, i.e., the 2nd subproblem that is associated with $\mathbf{w}^2$. Table I summarizes the percentage of the generalized subproblem preference regions over the feasible objective space.

Tuning $c(\mathbf{w})$ can adjust subproblem preference regions so that more update chances can be assigned to the subproblems of more interest and accelerate their convergence. For example, MOEA/D is tested on bi-objective ZDT4 [27] and DTLZ4 problems [28] with three subproblems illustrated in Fig. 2. The widely used simulated binary crossover (SBX) and polynomial mutation [29] are applied to generate offspring. With different settings of $c(\mathbf{w})$, the 1st subproblem associated with $\mathbf{w}^1$ possesses the largest preference region, as shown in Fig. 2 (a), and converges fastest, as shown in Figs. 3 (a) and (b), when $c(\mathbf{w}) = \|\mathbf{w}\|_{0.1}^4$. Similarly, the 2nd subproblem with $c(\mathbf{w}) = \|\mathbf{w}\|_{1.5}^4$ is assigned the largest preference region among the three cases as shown in Fig. 2 and reaches the fastest convergence rate as shown in Figs. 3 (c) and (d). The observations suggest that a subproblem with a larger preference region is likely updated more frequently and improved more often, which consequentially leads to faster convergence.

2) Improving the uniformity in partitioning the improvement region of all subproblems: To explain this point, a definition of subproblem improvement region based on maximal fitness improvement criterion is firstly introduced as follows:

$$\Psi^i = \{\mathbf{F}(\mathbf{y}) | \mathbf{y} \in \Omega, g(\mathbf{F}(\mathbf{y})|\mathbf{w}^i, \mathbf{z}^*) < g(\mathbf{F}(\mathbf{x}^i)|\mathbf{w}^i, \mathbf{z}^*), \\ i = \arg\max_{1 \le j \le N} \{c(\mathbf{w}) \cdot [g(\mathbf{F}(\mathbf{x}^i)|\mathbf{w}^j, \mathbf{z}^*) - g(\mathbf{F}(\mathbf{y})|\mathbf{w}^j, \mathbf{z}^*)]\}\} \tag{15}$$

where $\mathbf{x}^i$ is the current solution of the i-th subproblem. The inequality $g(\mathbf{F}(\mathbf{y})|\mathbf{w}^i, \mathbf{z}^*) < g(\mathbf{F}(\mathbf{x})|\mathbf{w}^i, \mathbf{z}^*)$ indicates that the offspring $\mathbf{y}$ obtains better fitness than the current solution $\mathbf{x}$ in the i-th subproblem. The last constraint in (15) identifies the subproblem where maximal fitness improvement is achieved.

An example of the improvement region of all subproblems is shown in Fig. 4 (d). The effect of $c(\mathbf{w})$ on partitioning the improvement region of all subproblems is shown in Figs. 4 (a)-(c) using (15) and the modified Tchebycheff decomposition. $c(\mathbf{w}) = \|\mathbf{w}\|_p$ is used and p is set to 1/3, 1, and 3 in Figs. 4 (a)-(c), respectively. It is shown that increasing p value improves the uniformity in partitioning the improvement region of all subproblems. This phenomenon is more obvious in the boundary regions, i.e., Ψ^1 and Ψ^4 in Figs. 4 (a)-(c), of the feasible objective space.

With $c(\mathbf{w})$, the algorithm is capable of tuning the uniformity of the improvement regions to improve the performance of the algorithm. A simple case is shown in Figs. 4 (a)-(c) where four uniform subproblems with different settings of $c(\mathbf{w})$ are evolved in MOEA/D. Bi-objective ZDT4 and DTLZ4 problems are selected as the test problems. Polynomial mutation and SBX are applied to generate offspring. The current solution of the i-th subproblem is updated by the offspring $\mathbf{y}$ if its corresponding objective vector is located in Ψ^i. Uniform partition of improvement regions leads to better general performance of all subproblems, as shown in Figs. 4 (e) and (f).

IV. POPULATION UPDATE STRATEGY BASED ON MAXIMAL FITNESS IMPROVEMENT

Population update strategy is a key component of MOEAs and has been extensively studied in the last few years. For example, MOEA/D based on differential evolution (MOEA/D-DE) [17] limits the number of improvable parent solutions updated by an offspring solution. MOEA/D with an adaptive global replacement (MOEA/D-AGR) [19] replaces parent solution(s) with a newly generated offspring solution based on the minimal function value. Stable matching model-based MOEA/D (MOEA/D-STM) [30] utilizes a stable matching model to pair each subproblem with one single solution when updating the population such that different subproblems have different solutions. To enhance the diversity of population, [31] further proposed interrelationship-based selection to select the elite solutions to survive in the evolution process. MOEA/D based on a generalized resource allocation strategy (MOEA/D-GRA) [32] updates subproblem solutions using a global replacement strategy. These population update strategies have successfully improved the performance of MOEA/D, however, most of them are designed to optimize the performance of only a portion of subproblems [17, 19, 32].

To improve the performance of the algorithm, this work proposes a global population update strategy based on maximal

This article has been accepted for publication in a future issue of this journal, but has not been fully edited. Content may change prior to final publication. Citation information: DOI 10.1109/TEVC.2017.2704118, IEEE Transactions on Evolutionary Computation

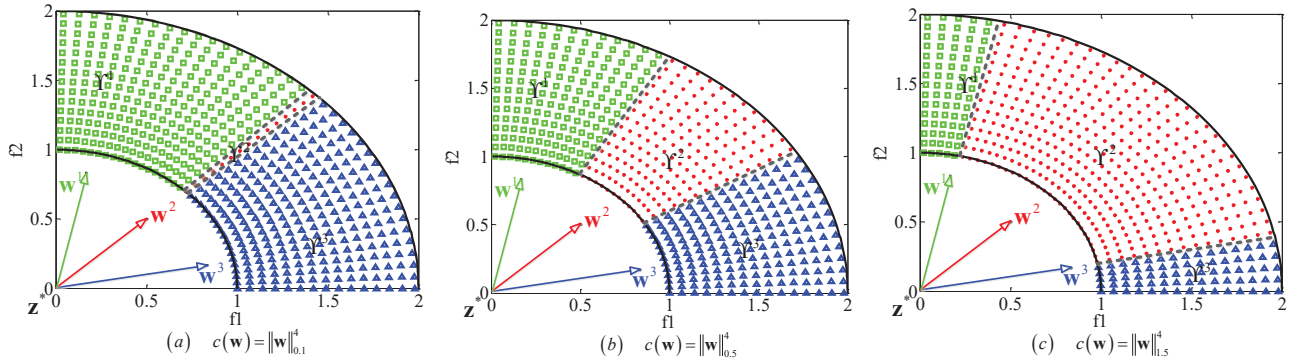

Fig. 2. Generalized subproblem preference region based on (a) $c(\mathbf{w}) = \|\mathbf{w}\|_{0.1}^4$, (b) $c(\mathbf{w}) = \|\mathbf{w}\|_{0.5}^4$, and (c) $c(\mathbf{w}) = \|\mathbf{w}\|_{1.5}^4$. The ideal point $\mathbf{z}^*$ is $(0,0)$ and the weight vector set is $\{\mathbf{w}^1, \mathbf{w}^2, \mathbf{w}^3\}$ with $\mathbf{w}^1 = (1/6, 5/6)$, $\mathbf{w}^2 = (1/2, 1/2)$, and $\mathbf{w}^3 = (5/6, 1/6)$. The feasible objective space $\mathbf{F}(\Omega)$ is $\{\mathbf{F} = (f_1, f_2) | 1 \leq \|\mathbf{F} - \mathbf{z}^*\|_2 \leq 2\}$.

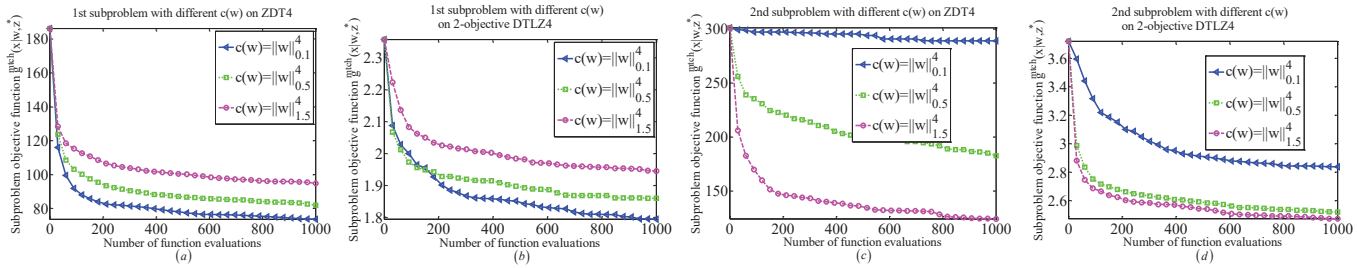

Fig. 3. Evolution process of (a) the 1st subproblem on ZDT4 problem, (b) the 1st subproblem on two objective DTLZ4 problem, (c) the 2nd subproblem on ZDT4 problem, and (d) the 2nd subproblem on two objective DTLZ4 problem. MOEA/D evolves only three subproblems whose weight vectors are $\mathbf{w}^1 = (1/6, 5/6)$, $\mathbf{w}^2 = (1/2, 1/2)$, and $\mathbf{w}^3 = (5/6, 1/6)$, respectively. Only offspring located on the preference region Υ^i as defined in (14) are able to update the i-th subproblem. The maximal number of function evaluations is set to 1,000.

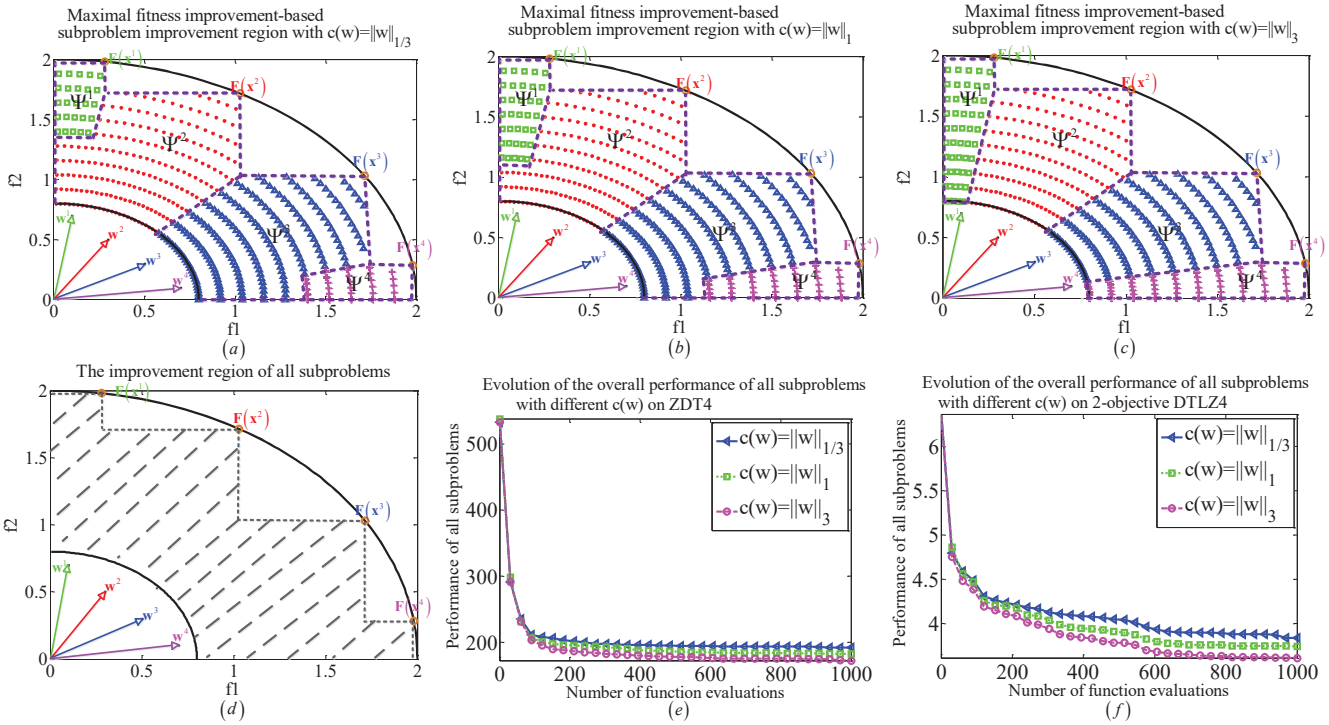

Fig. 4. Partitioning the improvement region of all subproblems using maximal fitness improvement criterion for Tchebycheff decompositions with (a) $l_{1/3}$-norm constraint on direction vectors, (b) l_1-norm constraint on direction vectors, and (c) l_3-norm constraint on direction vectors. (d) The improvement region of all subproblems shown in shadow area. The ideal point $\mathbf{z}^* = (0,0)$ and the weight vector set is $\{\mathbf{w}^1, \mathbf{w}^2, \mathbf{w}^3, \mathbf{w}^4\}$ with $\mathbf{w}^1 = (1/8, 7/8)$, $\mathbf{w}^2 = (3/8, 5/8)$, $\mathbf{w}^3 = (5/8, 3/8)$, and $\mathbf{w}^4 = (7/8, 1/8)$. $\mathbf{F}(\mathbf{x}^i) = 2\mathbf{w}^i / \|\mathbf{w}^i\|_2, i = 1, ..., 4$. The feasible objective set $\mathbf{F}(\Omega)$ is $\{\mathbf{F} = (f_1, f_2) | 0.8 \leq \|\mathbf{F} - \mathbf{z}^*\|_2 \leq 2\}$. Evolution process of the general performance of all subproblems on (e) ZDT4 problem, and (f) two objective DTLZ4 problem. Only offspring located on Ψ^i defined in (15) is able to update i-th subproblem. The maximal number of function evaluations is set to 1,000.

fitness improvement as outlined in Algorithm 1. Particularly, given a generated offspring $\mathbf{y}$ for the target subproblem, in the first two steps of Algorithm 1, the l-th subproblem in which $\mathbf{y}$ obtains the maximum fitness improvement is identified with

$$l = \arg\max_{1\leq i\leq N}\{g^{ptch}(\mathbf{F}(\mathbf{x}^i)|\boldsymbol{\lambda}^i,\mathbf{z}^*) - g^{ptch}(\mathbf{F}(\mathbf{y})|\boldsymbol{\lambda}^i,\mathbf{z}^*)\} \tag{16}$$

Afterward, in Step 3, the corresponding solution $\mathbf{x}^l$ is replaced by $\mathbf{y}$, if $\mathbf{y}$ performs better than $\mathbf{x}^l$ in the l-th subproblem. Finally, to improve the robustness of the proposed algorithm, a few parent solutions (no more than a predefined number $n_r - 1$) are also randomly selected and replaced by $\mathbf{y}$ in Step 4. The effects of using different p-Tchs are investigated in the experimental study based on the following equation:

$$g^{ptch}(\mathbf{F}(\mathbf{x}^i)|\boldsymbol{\lambda}^i,\mathbf{z}) - g^{ptch}(\mathbf{F}(\mathbf{y})|\boldsymbol{\lambda}^i,\mathbf{z}) \overset{(13)}{\underset{\mathbf{w}^i=\boldsymbol{\lambda}^i/\|\boldsymbol{\lambda}^i\|_1}{=\!=\!=}} \|\mathbf{w}^i\|_p \cdot [g^{mtch}(\mathbf{F}(\mathbf{x}^i)|\mathbf{w}^i,\mathbf{z}) - g^{mtch}(\mathbf{F}(\mathbf{y})|\mathbf{w}^i,\mathbf{z})]$$

The population update strategy outlined in Algorithm 1 is based on p-Tch yet 2-Tch is used in the experimental study. The reason of selecting $p = 2$ is that firstly p should be greater than 1 to improve the uniformity of the subproblem update regions, and secondly $p = 2$ is more favorable than $p > 2$ because the subproblem objective function in 2-Tch has a clearer geometric property in terms of Euclidean distance than that of using larger p values. A subproblem of 2-Tch is defined as follows:

$$\min_{\mathbf{x}\in\Omega} g^{2tch}(\mathbf{F}(\mathbf{x})|\boldsymbol{\lambda},\mathbf{z}^*) = \max_{1\leq i\leq m}\left\{\frac{f_i(\mathbf{x}) - z_i^*}{\lambda_i}\right\} \tag{17}$$

where $\boldsymbol{\lambda} = (\lambda_1,\ldots,\lambda_m)$ with $\|\boldsymbol{\lambda}\|_2 = 1$ and $\lambda_1,\ldots,\lambda_m \geq 0$.

In Algorithm 1, the fitness improvement is calculated with $g^{ptch}(\mathbf{F}(\mathbf{x}^i)|\boldsymbol{\lambda}^i,\mathbf{z}) - g^{ptch}(\mathbf{F}(\mathbf{y})|\boldsymbol{\lambda}^i,\mathbf{z})$. The corresponding geometric property of this fitness improvement in 2-Tch is shown in Fig. 5. According to *Proposition* 3.2, the fitness improvement is calculated as follows:

$$\begin{aligned} &g^{2tch}(\mathbf{F}(\mathbf{x}^i)|\boldsymbol{\lambda}^i,\mathbf{z}) - g^{2tch}(\mathbf{F}(\mathbf{y})|\boldsymbol{\lambda}^i,\mathbf{z}) \\ =&\|\bar{\mathbf{F}}(\mathbf{x}^i) - \mathbf{z}\|_2 - \|\bar{\mathbf{F}}(\mathbf{y}) - \mathbf{z}\|_2 = \|\bar{\mathbf{F}}(\mathbf{x}^i) - \bar{\mathbf{F}}(\mathbf{y})\|_2 \end{aligned}$$

where

$$\begin{aligned} \bar{\mathbf{F}}(\mathbf{x}^i) &= \mathbf{z} + g^{2tch}(\mathbf{F}(\mathbf{x}^i)|\boldsymbol{\lambda}^i,\mathbf{z})\cdot\boldsymbol{\lambda}^i \\ \bar{\mathbf{F}}(\mathbf{y}) &= \mathbf{z} + g^{2tch}(\mathbf{F}(\mathbf{y})|\boldsymbol{\lambda}^i,\mathbf{z})\cdot\boldsymbol{\lambda}^i \end{aligned}$$

That is actually the distance from $\bar{\mathbf{F}}(\mathbf{y})$ to $\bar{\mathbf{F}}(\mathbf{x}^i)$ as shown in Fig. 5.

Compared to the two other representative strategies namely the strategy based on minimal fitness value that is used in MOEA/D-AGR and the random improvable strategy used in MOEA/D, the proposed strategy based on maximal fitness improvement has the following strengths:

1) Good offspring individuals tend to survive longer in the proposed strategy. To explain this point, the difference between the fitness improvement and the fitness value is firstly illustrated in Fig. 6 using a bi-objective optimization problem. For example, after updating a particular subproblem i with an offspring $\mathbf{y}$, the corresponding fitness improvement

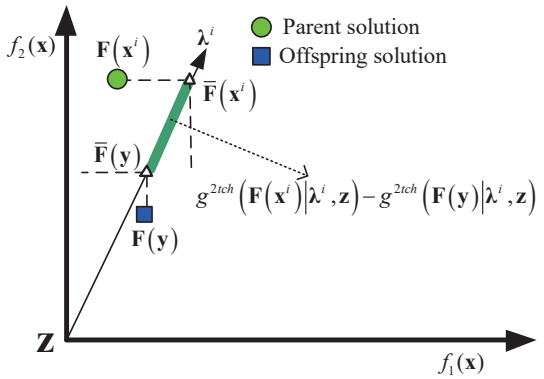

Fig. 5. The geometric property of fitness improvement $g^{2tch}(\mathbf{F}(\mathbf{x}^i)|\boldsymbol{\lambda}^i,\mathbf{z}) - g^{2tch}(\mathbf{F}(\mathbf{y})|\boldsymbol{\lambda}^i,\mathbf{z})$.

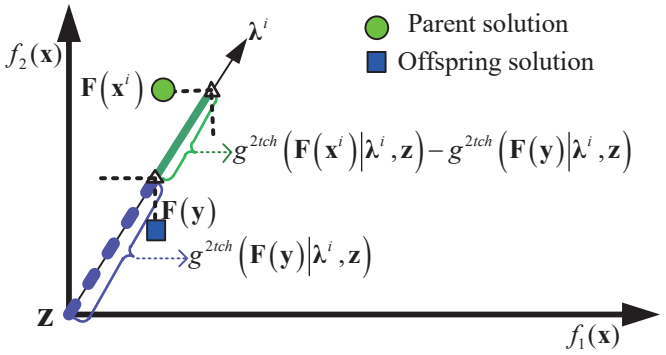

Fig. 6. The difference between the fitness improvement $g^{2tch}(\mathbf{F}(\mathbf{x}^i)|\boldsymbol{\lambda}^i,\mathbf{z}) - g^{2tch}(\mathbf{F}(\mathbf{y})|\boldsymbol{\lambda}^i,\mathbf{z})$ and the fitness value $g^{2tch}(\mathbf{F}(\mathbf{y})|\boldsymbol{\lambda}^i,\mathbf{z})$.

$g^{2tch}(\mathbf{F}(\mathbf{x}^i)|\boldsymbol{\lambda}^i,\mathbf{z}) - g^{2tch}(\mathbf{F}(\mathbf{y})|\boldsymbol{\lambda}^i,\mathbf{z})$ and the new fitness value $g^{2tch}(\mathbf{F}(\mathbf{y})|\boldsymbol{\lambda}^i,\mathbf{z})$ are shown as the solid and dotted line segments, respectively. Following the annotation of Fig. 6, a two-step example is further provided in Fig. 7 to distinguish the working processes of the three population update strategies. Particularly, two promising offspring solutions namely $\mathbf{y}$ and $\mathbf{y}^1$ are generated and applied to update the population in a row.

In the example shown in Fig. 7 (a), the first promising offspring solution $\mathbf{y}$ dominates three parent solutions namely $\mathbf{x}^2$, $\mathbf{x}^3$, and $\mathbf{x}^4$. Solution $\mathbf{y}$ achieves both the maximal fitness improvement and the minimal fitness value in the 3rd subproblem because of

$$\begin{aligned} &\arg\max_{1\leq i\leq 5}[g^{2tch}(\mathbf{F}(\mathbf{x}^i)|\boldsymbol{\lambda}^i,\mathbf{z}) - g^{2tch}(\mathbf{F}(\mathbf{y})|\boldsymbol{\lambda}^i,\mathbf{z})] = 3, \\ &\arg\min_{1\leq i\leq 5} g^{2tch}(\mathbf{F}(\mathbf{y})|\boldsymbol{\lambda}^i,\mathbf{z}) = 3 \end{aligned}$$

Hence, in the first step, the population update strategies based on maximal fitness improvement and minimal fitness value update $\mathbf{x}^3$ with offspring $\mathbf{y}$ as shown in Figs. 7 (b) and (d), respectively. The strategy used in MOEA/D randomly replaces an improvable parent individual like $\mathbf{x}^2$ as shown in Fig. 7(f). For the sake of clarity, a newly generated offspring solution $\mathbf{y}$ is used to replace at most one parent solution, i.e., $n_r = 1$, in Fig. 7. In the second step, given the second promising offspring solution $\mathbf{y}^1$ as shown in Figs. 7 (b), (d), and (f), the three strategies replace $\mathbf{x}^4$, $\mathbf{x}^3$, and $\mathbf{x}^2$ with $\mathbf{y}^1$ as shown in

Algorithm 1 Replacing parent solutions based on maximal fitness improvement

Require: j: index of the selected subproblem for reproduction.
$Neigh_j$:indices of the neighbor subproblems of the j-th subproblem, $Neigh_j = B^j = \{j_1, \ldots, j_T\}$ or $Neigh_j = \{1, \ldots, N\}$.
N: size of the evolutionary population. $\mathbf{y}$: newly generated offspring. $\mathbf{z}$: reference point.
$\boldsymbol{\lambda}^i, \mathbf{x}^i, \mathbf{F}^i$: direction vector, current decision vector and its objective function values of i-th subproblem.
n_r: maximum number of the replaced parent solutions by one offspring solution.
Step 1 Initialization: $c = 0, MaxFitImp = -\infty, l = -1$.
Step 2 Identify the subproblem of maximal fitness improvment.
For $i = 1$ to N **do**
2.1 $ImpVal = g^{ptch}(\mathbf{F}(\mathbf{x}^i)|\boldsymbol{\lambda}^i, \mathbf{z}) - g^{ptch}(\mathbf{F}(\mathbf{y})|\boldsymbol{\lambda}^i, \mathbf{z})$.
2.2 **If** $ImpVal > MaxFitImp$, **then** $MaxFitImp = ImpVal$ and $l = i$.
End of For
Step 3 Replace a parent solution: If $MaxFitImp > 0$, **then** set $\mathbf{x}^l = \mathbf{y}, \mathbf{F}^l = \mathbf{F}(\mathbf{y})$ and $c = c + 1$.
Step 4 Replace improvable parent solutions randomly
While $c < n_r \wedge Neigh_j \neq \emptyset$ **do**
4.1 Randomly select an index i from $Neigh_j$.
4.2 **If** $g^{ptch}(\mathbf{F}(\mathbf{x}^i)|\boldsymbol{\lambda}^i, \mathbf{z}) - g^{ptch}(\mathbf{F}(\mathbf{y})|\boldsymbol{\lambda}^i, \mathbf{z}) > 0$, **then** set $\mathbf{x}^i = \mathbf{y}, \mathbf{F}^i = \mathbf{F}(\mathbf{y})$ and $c = c + 1$.
4.3 Delete i from $Neigh_j$: $Neigh_j = Neigh_j \backslash \{i\}$.
End of While

Figs. 7 (c), (e), and (g), respectively. The reason lies in

$$\arg\max_{1 \leq i \leq 5} [g^{2tch}(\mathbf{F}(\mathbf{x}^i)|\boldsymbol{\lambda}^i, \mathbf{z}) - g^{2tch}(\mathbf{F}(\mathbf{y})|\boldsymbol{\lambda}^i, \mathbf{z})] = 4,$$
$$\arg\min_{1 \leq i \leq 5} g^{2tch}(\mathbf{F}(\mathbf{y})|\boldsymbol{\lambda}^i, \mathbf{z}) = 3$$

The update strategy used in MOEA/D can randomly replace $\mathbf{x}^2$ or $\mathbf{x}^3$ with $\mathbf{y}^1$ in Fig. 7 (f). Fig. 7 (g) assumes that $\mathbf{x}^2$ is replaced by $\mathbf{y}^1$. It is observed that the proposed strategy based on maximal fitness improvement successfully maintains the first promising individual $\mathbf{y}$, i.e., $\mathbf{x}^3$ in Fig. 7 (c), whereas the two other strategies discard $\mathbf{y}$ as shown in Figs. 7 (e) and (g). In other words, good solutions are more likely to survive in the proposed update strategy.

2) The proposed strategy improves the general performance on all subproblems, i.e., $\sum_{i=1}^{N} g^{2tch}(\mathbf{F}(\mathbf{x}^i)|\boldsymbol{\lambda}^i, \mathbf{z}^*)$, rather than a portion of subproblems. The rationale of using $\sum_{i=1}^{N} g^{2tch}(\mathbf{F}(\mathbf{x}^i)|\boldsymbol{\lambda}^i, \mathbf{z}^*)$ to estimate the performance of the whole population will also be explained in the definition of R_2^{2tch} indicator (20) in Section VI.

Given a population $\mathbf{A} = \{\mathbf{x}^1, \ldots, \mathbf{x}^N\}$, it is reasonable to assume that

$$g^{2tch}(\mathbf{F}(\mathbf{x}^i)|\boldsymbol{\lambda}^i, \mathbf{z}^*) = \min_{\mathbf{F}(\mathbf{x}) \in \mathbf{A}} \{g^{2tch}(\mathbf{F}(\mathbf{x})|\boldsymbol{\lambda}^i, \mathbf{z}^*)\}$$

where $\mathbf{x}^i$ is the best current solution of the i-th subproblem in MOEA/D. The ideal objective vector $\mathbf{z}^*$ is normally unknown in advance, so an estimation of $\mathbf{z}^*$ with a reference point $\mathbf{z}$ proposed in [3] is used in this study. The general performance of all subproblems can then be approximated by summing up the fitness values of all individuals in $\mathbf{A}$, i.e.,

$$g^{2tch}(\mathbf{F}(\mathbf{A})|\mathbf{D}, \mathbf{z}) = \sum_{i=1}^{N} g^{2tch}(\mathbf{F}(\mathbf{x}^i)|\boldsymbol{\lambda}^i, \mathbf{z})$$

where $\mathbf{D} = \{\boldsymbol{\lambda}^1, \ldots, \boldsymbol{\lambda}^N\}$ and the smaller $g^{2tch}(\mathbf{F}(\mathbf{A})|\mathbf{D}, \mathbf{z})$ suggests the better general performance on the whole population or all subproblems.

Let all the three compared strategies start from the same initial population $\mathbf{A}$ and a newly generated offspring solution $\mathbf{y}$ be used to replace only one parent solution. Without loss of generality, the proposed strategy based on maximal fitness improvement is supposed to update the l-th subproblem, while the two other strategies update the j-th subproblem. According to the definition of maximal fitness improvement in (16), it is obvious that

$$g^{2tch}(\mathbf{F}(\mathbf{x}^l)|\boldsymbol{\lambda}^l, \mathbf{z}) - g^{2tch}(\mathbf{F}(\mathbf{y})|\boldsymbol{\lambda}^l, \mathbf{z}) \geq g^{2tch}(\mathbf{F}(\mathbf{x}^j)|\boldsymbol{\lambda}^j, \mathbf{z}) - g^{2tch}(\mathbf{F}(\mathbf{y})|\boldsymbol{\lambda}^j, \mathbf{z})$$

Accordingly, the summarized fitness of the new population by updating the l-th subproblem is less than or equal to that of updating the j-th subproblem, i.e.,

$$g^{2tch}(\mathbf{F}(\mathbf{A})|\mathbf{D}, \mathbf{z}) - g^{2tch}(\mathbf{F}(\mathbf{x}^l)|\boldsymbol{\lambda}^l, \mathbf{z}) + g^{2tch}(\mathbf{F}(\mathbf{y})|\boldsymbol{\lambda}^l, \mathbf{z}) \leq g^{2tch}(\mathbf{F}(\mathbf{A})|\mathbf{D}, \mathbf{z}) - g^{2tch}(\mathbf{F}(\mathbf{x}^j)|\boldsymbol{\lambda}^j, \mathbf{z}) + g^{2tch}(\mathbf{F}(\mathbf{y})|\boldsymbol{\lambda}^j, \mathbf{z})$$

In other words, the proposed strategy can obtain better general performance on all subproblems than the two other population update strategies used in MOEA/D and MOEA/D-AGR.

V. Details of the Proposed MOEA/D-2TCHMFI

The 2-Tch and the proposed population update strategy based on maximal fitness improvement are integrated into the MOEA/D framework to form a new algorithm namely MOEA/D-2TCHMFI. MOEA/D-2TCHMFI, aiming to improve MOEA/D in terms of solution convergence, is outlined in Algorithm 2. Selection of the weight vectors/direction vectors is the key to find uniformly distributed solutions over PF. An optimal distribution of weights for a certain decomposition method can be obtained following [5–7], if the PF geometry of an MOP is known *a priori* and a clear definition of well distributed Pareto-optimal solutions is provided.

This article has been accepted for publication in a future issue of this journal, but has not been fully edited. Content may change prior to final publication. Citation information: DOI 10.1109/TEVC.2017.2704118, IEEE Transactions on Evolutionary Computation

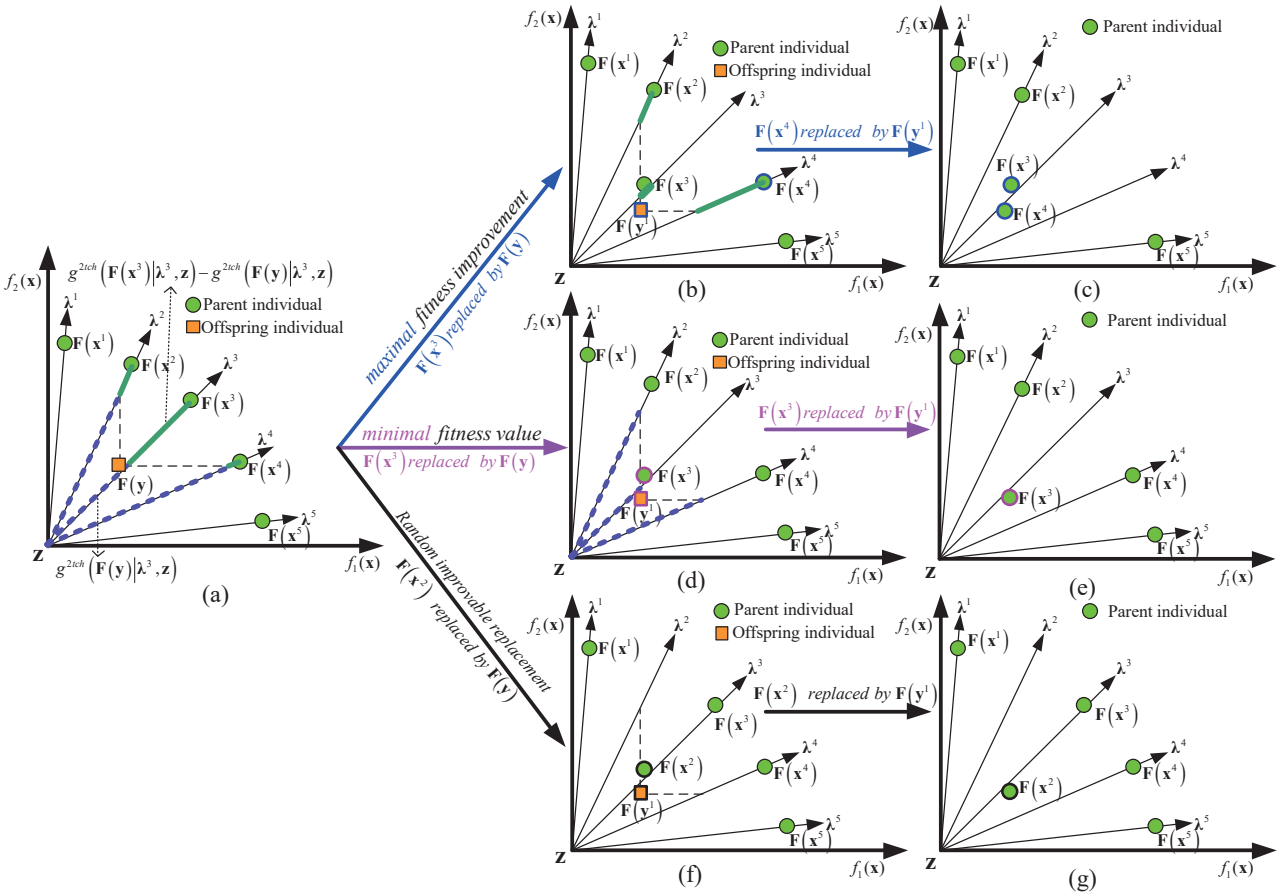

Fig. 7. Comparison of the three population update strategies with a bi-objective problem. (a) Five parent individuals and one offspring solution $\mathbf{y}$. (b) Replacement of $\mathbf{x}^3$ by $\mathbf{y}$ based on maximal fitness improvement criterion. (c) Replacement of $\mathbf{x}^2$ by $\mathbf{y}^1$ based on maximal fitness improvement criterion. (d) Replacement of $\mathbf{x}^3$ by $\mathbf{y}$ based on minimal fitness value criterion. (e) Replacement of $\mathbf{x}^3$ by $\mathbf{y}^1$ based on minimal fitness value criterion.(f) Replacement of $\mathbf{x}^2$ by $\mathbf{y}$ based on random improvable criterion. (g) Replacement of $\mathbf{x}^2$ by $\mathbf{y}^1$ based on random improvable criterion.

In Algorithm 2, Step 1 sets the direction vectors $\{\boldsymbol{\lambda}^1, ..., \boldsymbol{\lambda}^N\}$ as follows:

$$\boldsymbol{\lambda}^i = \frac{\mathbf{w}^i}{\|\mathbf{w}^i\|_2}, i = 1, \ldots, N$$

where $\{\mathbf{w}^1, ..., \mathbf{w}^N\}$ are uniformly distributed weight vectors generated by the method suggested in [3]. The uniform weight vectors $\{\mathbf{w}^1, ..., \mathbf{w}^N\}$ and their corresponding direction vectors $\{\boldsymbol{\lambda}^1, ..., \boldsymbol{\lambda}^N\}$ are visualized in Fig. 8. Step 2 selects merely $\lfloor N/5 \rfloor$ subproblems based on their recent performance for offspring reproduction in each generation. Step 3 iteratively evolves the chosen subproblems using 2-Tch and the population update strategy with maximal fitness improvement criterion. Particularly, in Step 3.1, each subproblem is optimized using information mainly from its neighbor subproblems. The reference point $\mathbf{z}$ is updated in Step 3.2 and the parent solutions are updated in Step 3.3 according to Algorithm 1. In Step 3.4, if the generation number gen is divisible by 30, the relative reduction of fitness value of the i-th subproblem in the last 30 generations is calculated as follows:

$$\triangle_i = \frac{g^{2tch}(\mathbf{F}(\mathbf{x}^{i,gen-30})|\boldsymbol{\lambda}^i, \mathbf{z}) - g^{2tch}(\mathbf{F}(\mathbf{x}^{i,gen})|\boldsymbol{\lambda}^i, \mathbf{z})}{g^{2tch}(\mathbf{F}(\mathbf{x}^{i,gen-30})|\boldsymbol{\lambda}^i, \mathbf{z})}$$

where $\mathbf{x}^{i,gen}$ and $\mathbf{x}^{i,gen-30}$ are the solutions of the i-th subproblem in the current generation and generation $gen-30$, respectively. Following [16], MOEA/D-2TCHMFI updates the utility of each subproblem $\pi_i, i = 1, ..., N$, based on $\triangle_i$ as follows:

$$\pi_i = \begin{cases} 1, & \text{if } \triangle_i > 0.001 \\ (0.95 + 0.05 \times \frac{\triangle_i}{0.001}) \times \pi_i, & \text{otherwise} \end{cases}$$

Finally, in Step 4, the algorithm is terminated if a predefined maximal number of fitness evaluations is reached.

VI. Unary R_2 Indicator Based on 2-Tch

To justify the efficiency of the proposed algorithm, a 2-Tch-based R_2 indicator is introduced in this section. R_2 indicator was firstly proposed by Hansen and Jaszkiewicz [15] in 1998. Recently, R_2 indicator has attracted increasing research interest [33–38]. Most studies [15, 34–38] of R_2 indicator are based on the conventional Tchebycheff decomposition and a few [33] are based on the modified Tchebycheff decomposition. Nevertheless, the geometric property of the R_2 indicator based on these two Tchebycheff decomposition approaches is not straightforward. Here, the new R_2 indicator showing clearer geometric property is proposed to approximate the hyper-

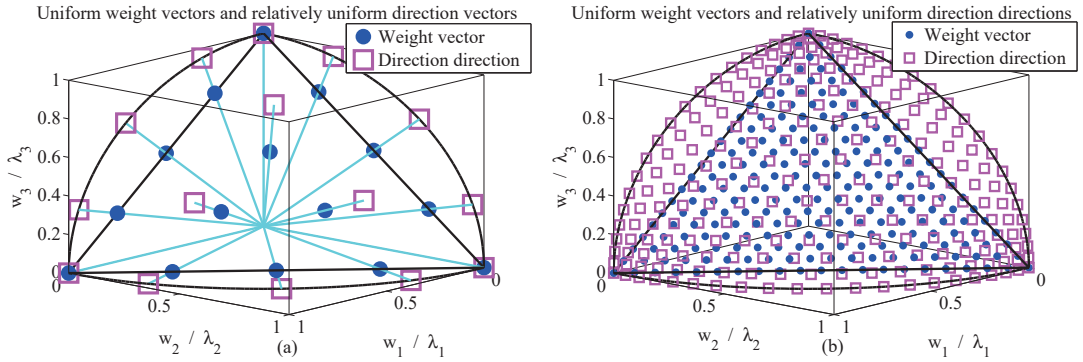

Fig. 8. The distribution of direction vectors with (a) a small size and (b) a large size.

Algorithm 2 MOEA/D-2TCHMFI

Require: m: number of individual functions defined in MOP (1),
N: population size, and T: number of neighbor subproblems.
Ensure: optimized population $\{\mathbf{x}^1,\ldots,\mathbf{x}^N\}$ and $\{\mathbf{F}^1,\ldots,\mathbf{F}^N\}$.

Step 1 Initialization

1.1 Initialize the population: generate $\{\mathbf{x}^1,\ldots,\mathbf{x}^N\}$ randomly, evaluate $\mathbf{F}^i=\mathbf{F}(\mathbf{x}^i), i=1,\ldots,N$, initialize the reference point $\mathbf{z}=(z_1,\ldots,z_m), z_i=\min\{f_i(\mathbf{x}^1),\ldots,f_i(\mathbf{x}^N)\}, i=1,...,m$, and set $gen=5$.

1.2 Initialize subproblems: evenly sample direction vectors $\{\boldsymbol{\lambda}^1,\ldots,\boldsymbol{\lambda}^N\}$, calculate $B^i=\{i_1,\ldots,i_T\}$ where $\{\boldsymbol{\lambda}^{i_1},\ldots,\boldsymbol{\lambda}^{i_T}\}$ are the T nearest direction vectors to $\boldsymbol{\lambda}^i$, and set utility of subproblems $u_i=1$, $i=1,\ldots,N$.

Step 2 Selection of subproblems to search: Initialize indices of m subproblems whose direction vectors are permutation of $(1,0,\ldots,0)$ as $Index$, apply tournament selection based on utilities $u_i, i=1,\ldots,N$, choose other $\lfloor\frac{N}{5}-m\rfloor$ indices, and add them to $Index$ [16].

Step 3 Evolution

For each $i\in Index$ **do**

3.1 Select neighborhood and generate offspring: If $rand()<0.9$, set $Neigh_i=B^i$. **Otherwise**, set $Neigh_i=\{1,2,\ldots,N\}$. Randomly choose two indices r_1 and r_2 from $Neigh_i$, and then generate a new solution $\mathbf{y}$ based on $\mathbf{x}^{r_1},\mathbf{x}^{r_2}$ and $\mathbf{x}^i$ by using evolutionary operators.

3.2 Update reference point z: For each $j=1,\ldots,m$, if $f_j(\mathbf{y})<z_j$, then set $z_j=f_j(\mathbf{y})$.

3.3 Update parent solutions with offspring y using Algorithms 1.

End of For

3.4 $gen++$. **If** $mod(gen,30)=0$, **then** update the utility of each subproblem [16].

Step 4 Stopping criterion: If the stopping criterion is reached, **then** stop and output $\{\mathbf{x}^1,\ldots,\mathbf{x}^N\}$ and $\{\mathbf{F}^1,\ldots,\mathbf{F}^N\}$. **Otherwise**, go to Step 2.

volume metric as follows:

$$R_2^{2tch}(\mathbf{A}|\mathbf{z}^*)=\frac{\int_{\boldsymbol{\lambda}\in\boldsymbol{\Lambda}}\min_{\mathbf{F}(\mathbf{x})\in A}\{g^{2tch}(\mathbf{F}(\mathbf{x})|\boldsymbol{\lambda},\mathbf{z}^*)\}d\boldsymbol{u}}{\int_{\boldsymbol{\Lambda}}d\boldsymbol{u}} \tag{18}$$

where

$$\boldsymbol{\Lambda}=\{\boldsymbol{\lambda}=(\lambda_1,\ldots,\lambda_m)|\lambda_i\geq 0, i=1,\ldots,m, \|\boldsymbol{\lambda}\|_2=1\} \tag{19}$$

and $d\boldsymbol{u}$ is the Lebesgue measure [39] on $\boldsymbol{\Lambda}$. Without the preference information of the decision-maker (DM), it is reasonable to assume that the direction vector $\boldsymbol{\lambda}$ obeys a uniform distribution over $\boldsymbol{\Lambda}$. $\int_{\boldsymbol{\Lambda}}d\boldsymbol{u}$ is equal to 2^{-m} times the surface area of an m-dimensional unit hyper-sphere since $\boldsymbol{\Lambda}$ is the part of unit hyper-sphere surface in the first quadrant, where m is the number of objective functions. The subproblem objective function $g^{2tch}(\mathbf{F}(\mathbf{x})|\boldsymbol{\lambda},\mathbf{z}^*)$ can be considered as a utility function/preference of the DM [20]. Given the options among all individuals in the population $\mathbf{A}$, the DM tends to choose the one with $\min_{\mathbf{F}(\mathbf{x})\in\mathbf{A}}\{g^{2tch}(\mathbf{F}(\mathbf{x})|\boldsymbol{\lambda},\mathbf{z}^*)\}$ as shown in Fig. 9 (a). The smaller $R_2^{2tch}(\mathbf{A}|\mathbf{z}^*)$ is, the better the expected utility/preference of DM is.

The geometric property of the proposed R_2^{2tch} metric is shown in Fig. 9 (b). Particularly, a point $\bar{\mathbf{P}}^i$ is introduced to facilitate the calculation of $\min_{\mathbf{F}(\mathbf{x})\in\mathbf{A}}\{g^{2tch}(\mathbf{F}(\mathbf{x})|\boldsymbol{\lambda}^i,\mathbf{z}^*)\}$, i.e.,

$$\min_{\mathbf{F}(\mathbf{x})\in\mathbf{A}}\{g^{2tch}(\mathbf{F}(\mathbf{x})|\boldsymbol{\lambda}^i,\mathbf{z}^*)\}=\|\bar{\mathbf{P}}^i-\mathbf{z}^*\|_2$$

It is easy to prove that:

$$\begin{aligned}R_2^{2tch}(\mathbf{A}|\mathbf{z}^*)&\approx\frac{\sum_{i=1}^{M}\min_{\mathbf{F}(\mathbf{x})\in\mathbf{A}}\{g^{2tch}(\mathbf{F}(\mathbf{x})|\boldsymbol{\lambda}^i,\mathbf{z}^*)\}}{M}\\&=\frac{\sum_{i=1}^{M}\|\bar{\mathbf{P}}^i-\mathbf{z}^*\|_2}{M}\end{aligned} \tag{20}$$

where M is the size of the direction vector set. Therefore, the geometric property of the proposed $R_2^{2tch}(\mathbf{A}|\mathbf{z}^*)$ indicator is actually the average length of the line segments that connect $\mathbf{z}^*$

and $\bar{\mathbf{P}}^i$. The distribution of $\bar{\mathbf{P}}^i$ fits well the surface of hyper-volume of the approximation set $\mathbf{A} = \{\mathbf{x}^1, \mathbf{x}^2, \mathbf{x}^3, \mathbf{x}^4\}$. As suggested in [35], $R_2^{2tch}(\mathbf{A}|\mathbf{z}^*)$ can be used to approximate the hyper-volume of set $\mathbf{A}$. A explanation of the simplified form in (20) is provided in Appendix A of the supplementary material. As proved in Appendix B of the supplementary material, the proposed unary indicator R_2^{2tch} (expected utility/preference of DM) is strictly monotonic with regard to Pareto dominance, which is critical for an evaluation indicator [40].

The superiority of the 2-Tch-based R_2 indicator to the two counterpart indicators based on the conventional Tchebycheff decomposition and the modified Tchebycheff decomposition is shown in Fig. 10. Let $R_2^{tch}(\mathbf{A}|\mathbf{z}^*)$ and $R_2^{mtch}(\mathbf{A}|\mathbf{z}^*)$ denote the two indicators using $g^{tch}(\mathbf{F}(\mathbf{x})|\mathbf{w}, \mathbf{z}^*)$ and $g^{mtch}(\mathbf{F}(\mathbf{x})|\mathbf{w}, \mathbf{z}^*)$ to replace $g^{2tch}(\mathbf{F}(\mathbf{x})|\boldsymbol{\lambda}, \mathbf{z}^*)$ in (18), respectively. Fig. 10 shows the geometric meanings of $R_2^{2tch}(\mathbf{A}|\mathbf{z}^*)$, $R_2^{mtch}(\mathbf{A}|\mathbf{z}^*)$, and $R_2^{tch}(\mathbf{A}|\mathbf{z}^*)$ in a bi-objective optimization problem. The geometric meanings of $R_2^{2tch}(\mathbf{A}|\mathbf{z}^*)$, $R_2^{tch}(\mathbf{A}|\mathbf{z}^*)$, and $R_2^{mtch}(\mathbf{A}|\mathbf{z}^*)$ are the average distances from the ideal point $\mathbf{z}^*$ to the curves 1, 2, and 3, respectively. It can be seen from Fig. 10 (a) that $R_2^{2tch}(\mathbf{A}|\mathbf{z}^*)$ represents the average distance from the ideal point $\mathbf{z}^*$ to the hyper-volume surface of the non-domination solution set. In contrast, neither $R_2^{tch}(\mathbf{A}|\mathbf{z}^*)$ nor $R_2^{mtch}(\mathbf{A}|\mathbf{z}^*)$ can show intuitive relationship with the distribution of the non-domination solution set as shown in Figs. 10 (b) and (c).

VII. Experimental studies

To test the performance of MOEA/D-2TCHMFI, we compare MOEA/D-2TCHMFI with other state-of-the-art MOEAs including the non-dominated-sorting-based NSGA-III [9], hyper-volume-based SMS-EMOA [41], MOEA/D with classical Tchebycheff decomposition (MOEA/D-TCH) [16], and MOEA/D with modified Tchebycheff decomposition (MOEA/D-MTCH) [9] using benchmark problems (including ZDT [27], DTLZ [28], and UF [42]) and two real-world flood control problems [23, 43, 44].

Polynomial mutation and simulated binary crossover (SBX) operator [29] are applied in continuous ZDT and DTLZ problems. Differential evolution (DE) and polynomial mutation [16] are used in UF1-UF13 problems. Following [3, 27, 28, 42], the dimension of the decision variable, the population size and the maximum number of function evaluations for different MOPs are summarized in Table II.

All algorithms are run on a workstation with Intel Core4 3.3 GHz CPU and 4 GB RAM. They are all terminated when the number of function evaluations reaches the predefined maximum value. The inverted generational distance (IGD) [40], additive ϵ-indicator (I_{ε^+}) [40] and R_2^{2tch} indicator defined in (18) are adopted to evaluate the performance of all compared algorithms.

1) IGD metric: Let $\mathbf{S}^*$ be a uniformly distributed solution set over the PF and $\hat{\mathbf{S}}$ be the approximate solutions found by an algorithm, the IGD metric, i.e., the mean distance from $\mathbf{S}^*$ to $\hat{\mathbf{S}}$ is calculated by:

$$IGD(\mathbf{S}^*, \hat{\mathbf{S}}) = \frac{\sum_{\mathbf{F} \in \mathbf{S}^*} d(\mathbf{F}, \hat{\mathbf{S}})}{|\mathbf{S}^*|}$$

TABLE II
Parameter setting for the selected MOPs, where m and n are the number of objective functions and decision variables, respectively.

m	n	MOP	Population size	maximum number of function evaluation
2	30 10	ZDT1-ZDT3 ZDT4,ZDT6	100	50,000
3	7 12 22	DTLZ1 DTLZ2-DTLZ4 DTLZ7	120	75,000
2 3 5	30	UF1-UF7 UF8-UF10 UF11-UF13	100 120 330	300,000
4	8 13	DTLZ1 DTLZ2-DTLZ4	165	400,000
5	9 14	DTLZ1 DTLZ2-DTLZ4	330	500,000
6	10 15	DTLZ1 DTLZ2-DTLZ4	462	600,000
2	12 25	Ankang20000712 Ankang20100715	100	100,000

where $d(\mathbf{F}, \hat{\mathbf{S}})$ is the minimal Euclidean distance from a Pareto-optimal solution $\mathbf{F}$ to the solutions in $\hat{\mathbf{S}}$. A low value of $IGD(\mathbf{S}^*, \hat{\mathbf{S}})$ indicates that the set $\hat{\mathbf{S}}$ is close to the entire Pareto-optimal front and covers the whole PF well. The reference sets $\mathbf{S}^*$ of many-objective DTLZ2-DTLZ4 problems can be generated following the construction of direction vectors presented in Section V and Fig. 8.

2) Additive ϵ-indicator I_{ε^+} [40]: Given two points $\mathbf{F}^1 = (f_1^1, ..., f_m^1)$ and $\mathbf{F}^2 = (f_1^2, ..., f_m^2)$ in an m-dimensional space,

$$\varepsilon^+(\mathbf{F}^1, \mathbf{F}^2) = \max_{1 \le i \le m} (f_i^2 - f_i^1)$$

defines the minimum value by which one needs to increase $\mathbf{F}^1$ in all coordinates such that it can be weakly dominated by $\mathbf{F}^2$. This value measures how well $\mathbf{F}^2$ approximates $\mathbf{F}^1$. For two sets $\mathbf{S}^*$ and $\hat{\mathbf{S}}$, I_{ε^+} is defined as follows:

$$I_{\varepsilon^+}(\mathbf{S}^*, \hat{\mathbf{S}}) = \max_{\mathbf{F}^1 \in \mathbf{S}^*} \min_{\mathbf{F}^2 \in \hat{\mathbf{S}}} \varepsilon^+(\mathbf{F}^1, \mathbf{F}^2)$$

The indicator accounts for the minimum value by which it needs to increase all points in $\mathbf{S}^*$ in all coordinates such that each point in $\mathbf{S}^*$ is dominated by some point in $\hat{\mathbf{S}}$, i.e., $I_{\varepsilon^+}(\mathbf{S}^*, \hat{\mathbf{S}})$ measures how well $\hat{\mathbf{S}}$ approximates $\mathbf{S}^*$.

3) R_2^{2tch} indicator is calculated based on the ideal objective vector $\mathbf{z}^* = (z_1^*, \ldots, z_m^*)$ and uniformly distributed preferred directions $\{\boldsymbol{\lambda}^1, \ldots, \boldsymbol{\lambda}^M\}$ (see Section VI). If the Pareto front of the target MOP is known in advance, the ideal objective vector is set to $z_i^* = \min\{f_i(\mathbf{x}^*), \mathbf{x}^* \in PS\}, i = 1, \ldots, m$. Let $\mathbf{S}^* = \{\mathbf{F}^1, \ldots, \mathbf{F}^M\}$ be a uniformly distributed solution set over the PF, the directions $\{\boldsymbol{\lambda}^1, \ldots, \boldsymbol{\lambda}^M\}$ can be generated with

$$\boldsymbol{\lambda}^i = \frac{\mathbf{F}^i - \mathbf{z}^*}{\|\mathbf{F}^i - \mathbf{z}^*\|_2}, i = 1, \ldots, M$$

If the PF of the target MOP is unknown, the approximate solutions found by all compared algorithms are used to evaluate the ideal objective vector $\mathbf{z}^*$. Preferred directions $\{\boldsymbol{\lambda}^1, \ldots, \boldsymbol{\lambda}^M\}$ are uniformly distributed over $\boldsymbol{\Lambda}$ as defined in (19). If the ideal point $\mathbf{z}^*$ is known in advance, $R_2^{2tch}(A|\mathbf{z}^*)$ is used, otherwise we suggest $R_2^{mtch}(A|\mathbf{r}) = \left[\int_{\boldsymbol{\lambda} \in \boldsymbol{\Lambda}} \max_{\mathbf{F}(\mathbf{x}) \in A} \{h(\mathbf{F}(\mathbf{x})|\boldsymbol{\lambda}, \mathbf{r})\} d\boldsymbol{u}\right] / \left[\int_{\boldsymbol{\Lambda}} d\boldsymbol{u}\right]$, where

This article has been accepted for publication in a future issue of this journal, but has not been fully edited. Content may change prior to final publication. Citation information: DOI 10.1109/TEVC.2017.2704118, IEEE Transactions on Evolutionary Computation

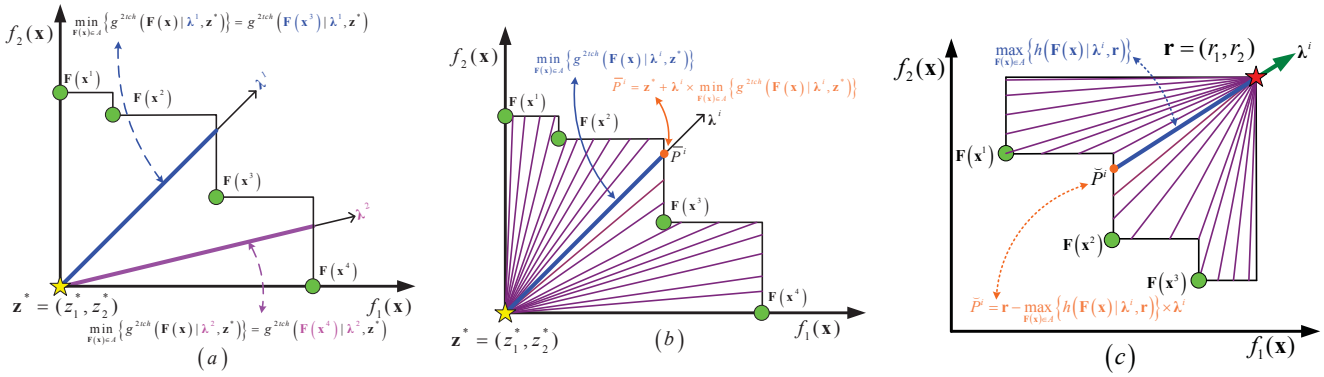

Fig. 9. (a) The geometric property of $\min_{\mathbf{F}(\mathbf{x})\in\mathbf{A}}\{g^{2tch}(\mathbf{F}(\mathbf{x})|\boldsymbol{\lambda},\mathbf{z}^*)\}$. (b) The geometric property of our proposed $R_2^{2tch}(\mathbf{A}|\mathbf{z}^*)$ metric. (c) The geometric property of the proposed $R_2^{2tch}(\mathbf{A}|\mathbf{r})$ metric.

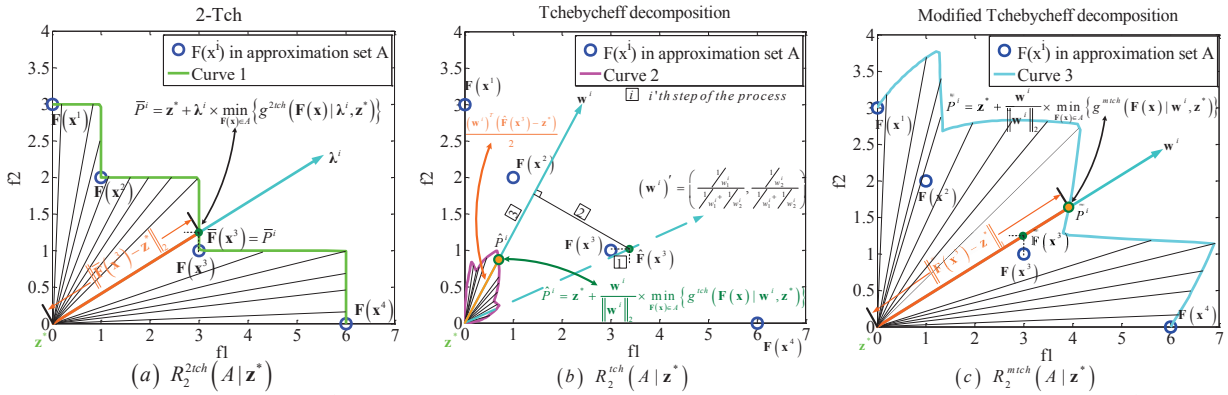

Fig. 10. (a) The geometric property of $R_2^{2tch}(A|\mathbf{z}^*)$ metric on bi-objective optimization problem. (b) The geometric property of $R_2^{mtch}(A|\mathbf{z}^*)$ metric. (c) The geometric property of $R_2^{tch}(A|\mathbf{z}^*)$ metric.

$h(\mathbf{F}(\mathbf{x})|\boldsymbol{\lambda},\mathbf{r}) = \min_{1\le i\le m}\{[r_i - f_i(\mathbf{x})]/\lambda_i\}$. The geometric property of the proposed metric $R_2^{ntch}(A|\mathbf{r})$ is shown in Fig. 9 (c). Reference point $\mathbf{r} = (r_1, ..., r_m)$ is set as

$$r_i = f_i^{min} + 1.1 \times (f_i^{max} - f_i^{min})$$

where f_i^{min} and f_i^{max} are the minimal and maximal objective values obtained by all compared algorithms in the i-th objective function $f_i(\mathbf{x})$, respectively.

To calculate the statistics of the three metrics, each compared algorithm is run for 30 times independently and the mean values are reported. The best performance among all compared algorithms is highlighted in bold face. Wilcoxon's rank sum test at 0.05 significance level is used to compare the differences between the best algorithm and the other algorithms. A superscript '+' is used to indicate the significant difference between the best algorithm and another compared algorithm.

A. MOEA/D-2TCHMFI vs. other state-of-the-art MOEAs on benchmark problems

The mean and standard deviation of $I_{\epsilon+}$-metric, IGD-metric and R_2^{2tch}-metric values of the solution sets obtained by all algorithms are reported in Table III. Table IV presents the statistical test results between MOEA/D-2TCHMFI and other compared algorithms. The results show that MOEA/D-2TCHMFI outperforms the other algorithms in most of the benchmark problems in terms of the three metrics. Fig. 11 shows the obtained solutions on the objective space and Fig. 12 reports the evolution process of the mean IGD-metric values. It is observed that MOEA/D-2TCHMFI obtains the best solutions in terms of convergence and uniformity on most of the benchmark problems.

Most of the ZDT and DTLZ problems are considered as simple MOPs due to the lack of linkages among decision variables [17, 45–47]. Generally, SMS-EMOA performs the best in bi-objective ZDT problems in that it uses hyper-volume metric to maintain the uniformity of evolutionary population. However, the uniformity of the found solutions by SMS-EMOA in tri-objective DTLZ problems deteriorates as shown in Fig. 11. The reason is that hyper-volume metric prefers the solutions on the boundary of PF, i.e., hyper-volume metric is sensitive to the extremal solutions. If the population size is limited, SMS-EMOA could not have sufficient solutions to cover the interior of PF especially in many-objective optimization problems.

NSGA-III obtains better solutions than MOEA/D-2TCHMFI, MOEA/D-MTCH, and MOEA/D-TCH in ZDT3 and DTLZ7 problems. In these MOPs with discontinuous PFs, MOEA/Ds tend to find redundant optimal solutions on the boundaries of PF due to the use of fixed weight vectors during the evolution [8, 47].

Since the objective functions of DTLZ2 problem are unimodal [46], it is easy for all MOEAs to approximate the PF.

DTLZ2 problem is a suitable benchmark to investigate the diversity preservation of the MOEAs. The obtained solutions of the compared algorithms are shown in Fig. 11. The solution set of MOEA/D-2TCHMFI is similar to that of MOEA/D-MTCH and NSGA-III, and better than that of MOEA/D-TCH and SMS-EMOA on DTLZ2 problem. The uniformity of the solution set obtained by MOEA/D-TCH is not as good as other methods.

UF problems are difficult to solve because their objective functions are not separable [23]. UF3, UF5 and UF10 problems have 8^{n-1},5^{n-1}, and 9^{n-2} local PFs, respectively, which poses big challenges to the MOEAs. As shown in Fig. 11, MOEA/D-2TCHMFI and MOEA/D-TCH are able to approximate the whole PF of UF3, whereas the solutions of the other three algorithms do not converge satisfactorily. All compared MOEAs fail to approximate the whole PF of UF5 due to its discontinuous nature. Nevertheless, as shown in Table III and Fig. 11, MOEA/D-2TCHMFI obtains better solutions than the other algorithms in terms of diversity and convergence. In the tri-objective UF10 problem, none of the compared MOEAs can find well-converged solutions. By using a neighborhood based search as described in Step 3.1 of Algorithm 2, MOEA/D-2TCHMFI, MOEA/D-MTCH, and MOEA/D-TCH obtain better solutions than NSGA-III and SMS-EMOA in term of convergence as shown in Table III and Fig. 11.

MOEA/D-2TCHMFI is observed to converge faster than all other compared algorithms in the early stage of the evolution and faster than the two decomposition-based algorithms, i.e., MOEA/D-TCH and MOEA/D-MTCH, throughout the whole evolution, on most of the benchmark problems as shown in Fig. 12.

The algorithms are also tested on many-objective problems and MOPs with preference information, in Appendixes C and D of the supplementary material, respectively, where MOEA/D-2TCHMFI shows superiority consistently. The effects of using $c(\mathbf{w}) = \|\mathbf{w}\|_p$ with different p values are investigated in Appendix E of the supplementary material and the results are consistent with the previously analysis in Fig. 4 and Section III-B. The selection of $p = 2$ is demonstrated to reach a good compromise of algorithm performance and ease of theocratical analysis.

B. Effectiveness of 2-Tch and the population update strategy based on maximal fitness improvement

To demonstrate the effectiveness of the proposed 2-Tch and the population update strategy based on maximal fitness improvement, MOEA/D-2TCHMFI is compared with MOEA/D-TCH, MOEA/D-MTCH, MOEA/D-2TCH (MOEA/D with merely 2-Tch, i.e., without using the new population update strategy), MOEA/D-TCHMFI (MOEA/D with conventional Tchebycheff decomposition and the new population update strategy), and MOEA/D-MTCHMFI (MOEA/D with the modified Tchebycheff decomposition and the new population update strategy).

The mean and standard deviation of IGD-metric and R_2^{2tch}-metric values of the solution sets obtained by all algorithms are reported in Table V. Table VI reports the statistical comparisons among these algorithms. According to Wilcoxon's rank sum test at 5% significance level, MOEA/D-2TCH significantly outperforms MOEA/D-TCH and MOEA/D-MTCH on most benchmark MOPs in terms of IGD-metric and R_2^{2tch}-metric. Similarly, MOEA/D-2TCHMFI preforms better than MOEA/D-TCHMFI and MOEA/D-MTCHMFI on most benchmark MOPs. The observations suggest that the proposed 2-Tch is more efficient and effective than the conventional Tchebycheff decomposition and the modified Tchebycheff decomposition w/o the new population update stragety.

TABLE VI
STATISTICS OF PERFORMANCE COMPARISONS AMONG MOEA/D-TCH, MOEA/D-MTCH, MOEA/D-2TCH, MOEA/D-TCHMFI, MOEA/D-MTCHMFI, AND MOEA/D-2TCHMFI BASED ON THE WILCOXON RANK SUM TEST AT A 5% SIGNIFICANCE LEVEL. "+", "≈"AND "-" RESPECTIVELY IS THE NUMBER OF ALGORITHM A IS BETTER THAN, SIMILAR TO, AND WORSE THAN ALGORITHM B FOR ALGORITHM A VERSUS ALGORITHM B.

	IGD			R_2^{2tch}		
	+	≈	-	+	≈	-
MOEA/D-2TCH vs. MOEA/D-TCH	19	0	1	16	1	3
MOEA/D-2TCHMFI vs. MOEA/D-TCHMFI	18	1	1	19	0	1
MOEA/D-TCHMFI vs. MOEA/D-TCH	17	1	2	14	1	5
MOEA/D-2TCHMFI vs. MOEA/D-2TCH	17	0	3	17	1	2
MOEA/D-2TCH vs. MOEA/D-MTCH	12	1	7	12	1	7
MOEA/D-2TCHMFI vs. MOEA/D-MTCHMFI	12	1	7	12	0	8
MOEA/D-MTCHMFI vs. MOEA/D-MTCH	13	2	5	13	1	6

With the new population update strategy, MOEA/D-TCHMFI, MOEA/D-MTCHMFI, and MOEA/D-2TCHMFI outperform their counterpart algorithms, i.e., MOEA/D-TCH, MOEA/D-MTCH, and MOEA/D-2TCH, respectively, on most benchmark MOPs in terms of IGD-metric and R_2^{2tch}-metric. The results demonstrate the effectiveness and efficiency of the proposed population update strategy based on maximal fitness improvement.

The 2-Tch has three advantages over the modified Tchebycheff decomposition (1-Tch): 1) The 2-Tch is more favorable for theoretical analysis thanks to its more intuitive geometric property as shown in Figs. 5 and 10; 2) the geometric property of $R_2^{2tch}(\mathbf{A}|\mathbf{z}^*)$ (R_2 indictor based on 2-Tch) is clearer than $R_2^{mtch}(\mathbf{A}|\mathbf{z}^*)$ (R_2 indictor based on 1-Tch) as shown in Figs. 10(a) and 10(c); 3) the uniformity of subproblem improvement regions with 2-Tch is better than that with 1-Tch as shown in Fig. 4. With the help of 2-Tch, the population update strategy based on maximal fitness improvement also manages to obtain better performance than other counterpart population update strategies.

C. Real-world application on reservoir flood control problems

In this subsection, the proposed algorithm is tested on real-world problems of reservoir flood control (RFC). The high occurrence frequency and immense destructive power of flood disaster make RFC an important problem worthy of research. RFC is a complex multi-objective optimization problem that has to consider various needs such as the security of reservoir during flood, the amount of electricity after flood, and the need of irrigation after flood [23, 44].

Let $\mathbf{Q} = (Q_1, \ldots, Q_T)$ be a decision vector of discharge volumes in T scheduling time intervals. The multi-objective

TABLE III

MEAN AND STANDARD DEVIATION OF IGD, $I_{\epsilon+}$, AND R_2^{2tch} METRIC VALUES ON MOPS. THE VALUE WITHIN PARENTHESES IS THE DEVIATION OF THE METRIC. THE BEST MEAN VALUE IS HIGHLIGHTED WITH BOLD AND THE SUBOPTIMAL MEAN VALUE IS HIGHLIGHTED IN BOLD, ITALIC AND UNDERLINE. BASED ON WILCOXON'S RANK SUM TEST AT 5% SIGNIFICANCE LEVEL, "+" IS THE PERFORMANCE OF BEST ALGORITHM ARE STATISTICALLY BETTER THAN OTHER COMPARED ALGORITHM.

Metric	MOEA/D-2TCHMFI			MOEA/D-TCH			NSGA-III			SMS-EMOA			MOEA/D-MTCH		
	IGD	$I_{\epsilon+}$	R_2^{2tch}	IGD	$I_{\epsilon+}$	R_2^{2tch}	IGD	$I_{\epsilon+}$	R_2^{2tch}	IGD	$I_{\epsilon+}$	R_2^{2tch}	IGD	$I_{\epsilon+}$	R_2^{2tch}
ZDT1	***4.616e-3***$^+$ (2.373e-5)	***1.180e-2***$^+$ (8.116e-5)	***6.793e-1***$^+$ (3.183e-3)	4.741e-3$^+$ (7.399e-5)	1.197e-2$^+$ (5.714e-4)	6.871e-1$^+$ (6.437e-3)	4.658e-3$^+$ (1.267e-4)	1.213e-2$^+$ (5.469e-4)	6.720e-1$^+$ (7.155e-4)	**3.619e-3** (2.332e-5)	**5.191e-3** (1.396e-4)	**6.698e-1** (1.862e-4)	4.709e-3$^+$ (3.849e-5)	1.188e-2$^+$ (8.560e-5)	6.829e-1$^+$ (4.406e-3)
ZDT2	**4.155e-3** (1.020e-5)	**8.892e-3** (1.414e-4)	**9.332e-1** (4.439e-3)	4.373e-3$^+$ (5.927e-5)	1.012e-2$^+$ (3.274e-4)	9.615e-1$^+$ (8.909e-3)	***4.185e-3***$^+$ (1.205e-5)	***9.408e-3***$^+$ (3.262e-4)	***9.358e-1***$^+$ (7.001e-4)	4.308e-3$^+$ (8.593e-5)	9.935e-3$^+$ (1.183e-4)	9.418e-1$^+$ (5.326e-4)	4.209e-3$^+$ (1.992e-5)	9.783e-3$^+$ (9.190e-4)	9.512e-1$^+$ (6.375e-3)
ZDT3	1.371e-2$^+$ (9.388e-5)	2.398e-2$^+$ (1.622e-4)	1.186$^+$ (3.077e-4)	1.376e-2$^+$ (2.564e-4)	2.403e-2$^+$ (4.445e-4)	1.189$^+$ (3.028e-3)	***6.977e-3***$^+$ (3.985e-4)	***1.049e-2***$^+$ (1.363e-3)	***1.176***$^+$ (8.615e-4)	**4.246e-3** (1.267e-5)	**3.397e-3** (1.652e-4)	**1.171** (4.986e-5)	1.374e-2$^+$ (9.908e-5)	2.400e-2$^+$ (2.248e-4)	1.187$^+$ (2.052e-3)
ZDT4	***4.793e-3***$^+$ (1.447e-4)	***1.305e-2***$^+$ (9.844e-4)	***6.844e-1***$^+$ (1.226e-2)	4.884e-3$^+$ (1.297e-4)	1.358e-2$^+$ (9.271e-4)	6.943e-1$^+$ (1.397e-2)	5.188e-3$^+$ (1.482e-3)	1.359e-2$^+$ (6.100e-3)	6.867e-1$^+$ (9.578e-3)	**3.724e-3** (1.259e-4)	**5.973e-3** (5.707e-4)	**6.786e-1** (6.134e-3)	4.815e-3$^+$ (1.386e-4)	1.302e-2$^+$ (9.280e-4)	6.868e-1$^+$ (1.228e-2)
ZDT6	***3.724e-3***$^+$ (1.084e-4)	***8.383e-3***$^+$ (2.356e-4)	***7.387e-1***$^+$ (6.449e-3)	4.657e-3$^+$ (3.741e-4)	1.118e-2$^+$ (1.428e-3)	7.713e-1$^+$ (1.667e-2)	4.397e-3$^+$ (2.648e-4)	1.043e-2$^+$ (4.593e-4)	7.539e-1$^+$ (1.885e-2)	**3.014e-3** (2.609e-5)	**4.557e-3** (1.354e-4)	**7.251e-1** (4.994e-3)	4.232e-3$^+$ (2.263e-4)	9.579e-3$^+$ (9.522e-4)	7.577e-1$^+$ (1.167e-2)
DTLZ1	**2.207e-2** (3.380e-3)	**4.490e-2** (5.389e-3)	**4.132e-1** (1.261e-2)	4.225e-2$^+$ (6.952e-2)	6.136e-2$^+$ (4.425e-2)	4.847e-1$^+$ (2.784e-2)	***2.274e-2***$^+$ (4.989e-3)	***4.601e-2***$^+$ (4.449e-3)	***4.180e-1***$^+$ (1.219e-2)	2.450e-2$^+$ (1.019e-4)	4.986e-2$^+$ (3.247e-3)	4.213e-1$^+$ (1.362e-3)	2.336e-2$^+$ (4.196e-2)	4.812e-2$^+$ (7.597e-3)	4.793e-1$^+$ (1.669e-1)
DTLZ2	**5.267e-2** (1.434e-4)	**7.563e-2** (2.952e-3)	**1.055** (2.187e-2)	6.165e-2$^+$ (3.839e-4)	1.259e-1$^+$ (2.673e-3)	1.106$^+$ (2.080e-2)	5.279e-2$^+$ (2.313e-4)	7.815e-2$^+$ (1.061e-2)	1.068$^+$ (1.040e-1)	6.637e-2$^+$ (3.395e-4)	7.917e-2$^+$ (3.072e-3)	1.078$^+$ (3.343e-4)	***5.278e-2***$^+$ (1.638e-4)	***7.740e-2***$^+$ (2.345e-3)	***1.061***$^+$ (2.995e-2)
DTLZ3	**5.333e-2** (5.819e-4)	**9.433e-2** (1.408e-2)	**1.158** (6.767e-2)	6.284e-2$^+$ (4.070e-3)	1.249e-1$^+$ (9.264e-3)	1.256$^+$ (1.486e-1)	6.651e-2$^+$ (2.191e-2)	1.091e-1$^+$ (4.193e-2)	***1.164***$^+$ (3.042e-2)	6.673e-2$^+$ (6.920e-4)	6.583e-2$^+$ (2.667e-3)	1.179$^+$ (2.227e-3)	***5.430e-2***$^+$ (1.624e-3)	***9.666e-2***$^+$ (1.340e-2)	1.343$^+$ (2.354e-1)
DTLZ4	**5.265e-2** (1.467e-4)	**7.492e-2** (8.613e-3)	**1.034** (3.466e-3)	6.194e-2$^+$ (3.736e-4)	1.261e-1$^+$ (2.229e-3)	1.071$^+$ (1.278e-2)	5.280e-2$^+$ (3.476e-3)	7.853e-2$^+$ (9.641e-3)	1.104$^+$ (2.375e-3)	2.125e-1$^+$ (2.351e-1)	2.593e-1$^+$ (3.093e-1)	1.497$^+$ (3.814e-1)	***5.266e-2***$^+$ (1.653e-4)	***7.504e-2***$^+$ (6.185e-3)	***1.039***$^+$ (1.421e-3)
DTLZ7	***1.130e-1***$^+$ (3.171e-3)	***1.353e-1***$^+$ (5.335e-4)	**2.416** (4.842e-2)	1.433e-1$^+$ (1.255e-3)	1.684e-1$^+$ (1.875e-3)	***2.437***$^+$ (6.814e-3)	**6.494e-2** (1.744e-3)	**1.194e-1** (8.991e-4)	2.475$^+$ (8.331e-2)	2.032e-1$^+$ (1.325e-1)	5.631e-1$^+$ (6.038e-1)	2.869$^+$ (7.051e-1)	1.137e-1$^+$ (3.340e-3)	1.354e-1$^+$ (8.706e-4)	2.444$^+$ (7.315e-2)
UF1	**6.113e-3** (3.431e-4)	**1.816e-2** (3.492e-3)	**7.090e-1** (1.192e-2)	7.265e-3$^+$ (1.555e-3)	2.649e-2$^+$ (1.045e-2)	7.105e-1$^+$ (1.349e-2)	1.382e-2$^+$ (2.287e-3)	3.082e-2$^+$ (8.540e-3)	7.629e-1$^+$ (5.836e-2)	1.323e-2$^+$ (6.417e-3)	4.381e-2$^+$ (3.139e-2)	7.143e-1$^+$ (9.912e-3)	***6.171e-3***$^+$ (3.937e-4)	***1.936e-2***$^+$ (4.486e-3)	***7.099e-1***$^+$ (1.027e-2)
UF2	**8.281e-3** (9.953e-4)	**2.998e-2** (8.127e-3)	**7.688e-1** (1.778e-1)	9.422e-3$^+$ (7.101e-4)	3.447e-2$^+$ (6.361e-3)	8.224e-1$^+$ (1.297e-1)	1.436e-2$^+$ (9.522e-4)	4.108e-2$^+$ (6.792e-3)	9.006e-1$^+$ (1.678e-1)	1.389e-2$^+$ (1.897e-3)	5.218e-2$^+$ (1.283e-2)	8.513e-1$^+$ (1.699e-1)	***8.425e-3***$^+$ (1.639e-3)	***3.111e-2***$^+$ (1.130e-2)	***7.915e-1***$^+$ (1.679e-1)
UF3	***1.256e-2***$^+$ (9.497e-3)	***4.361e-2***$^+$ (3.279e-2)	***8.305e-1***$^+$ (3.983e-1)	1.316e-2$^+$ (9.922e-3)	4.930e-2$^+$ (3.229e-2)	8.338e-1$^+$ (4.426e-1)	3.122e-2$^+$ (2.151e-2)	8.641e-2$^+$ (5.790e-2)	1.118$^+$ (6.253e-1)	3.872e-2$^+$ (2.692e-2)	9.560e-2$^+$ (4.427e-2)	1.290$^+$ (3.568e-1)	**9.478e-3** (5.180e-3)	**3.288e-2** (2.717e-2)	**8.239e-1** (4.207e-1)
UF4	**5.928e-2** (3.698e-3)	**7.308e-2** (6.950e-3)	**2.143** (1.455e-1)	6.411e-2$^+$ (4.917e-3)	8.127e-2$^+$ (7.997e-3)	2.273$^+$ (3.410e-1)	***6.195e-2***$^+$ (4.911e-3)	***8.020e-2***$^+$ (7.133e-3)	***2.168***$^+$ (1.559e-1)	6.865e-2$^+$ (9.592e-3)	8.400e-2$^+$ (4.719e-3)	2.205$^+$ (2.722e-1)	6.252e-2$^+$ (5.020e-3)	7.996e-2$^+$ (1.003e-2)	2.188$^+$ (2.045e-1)
UF5	**1.058e-1** (2.468e-2)	**2.030e-2** (5.139e-2)	**7.010** (6.016)	1.572e-1$^+$ (7.468e-2)	3.024e-1$^+$ (1.581e-1)	1.469e+1$^+$ (1.165e+1)	3.041e-1$^+$ (1.112e-1)	4.090e-1$^+$ (1.135e-1)	***1.254e+1***$^+$ (7.497)	4.991e-1$^+$ (1.562e-1)	6.476e-1$^+$ (9.560e-2)	1.802e+1$^+$ (8.902)	***1.473e-1***$^+$ (7.445e-2)	***2.827e-1***$^+$ (1.454e-1)	1.346e+1$^+$ (1.017e+1)
UF6	2.601e-1$^+$ (1.584e-1)	4.314e-1$^+$ (1.899e-1)	3.084$^+$ (2.216)	3.387e-1$^+$ (2.174e-1)	5.424e-1$^+$ (2.513e-1)	4.283$^+$ (2.306)	***1.787e-1***$^+$ (1.344e-1)	***3.614e-1***$^+$ (1.925e-1)	***2.080***$^+$ (7.513e-1)	**1.615e-1** (1.692e-1)	**3.182e-1** (2.397e-1)	**2.000** (1.047)	2.982e-1$^+$ (1.788e-1)	5.115e-1$^+$ (2.444e-1)	3.741$^+$ (1.953)
UF7	**6.192e-3** (2.454e-3)	**3.023e-2** (2.417e-2)	**9.233e-1** (1.260e-1)	7.571e-3$^+$ (2.164e-3)	4.013e-2$^+$ (2.205e-2)	9.892e-1$^+$ (2.070e-1)	1.077e-2$^+$ (1.919e-3)	5.247e-2$^+$ (1.677e-2)	1.130$^+$ (4.390e-1)	7.636e-3$^+$ (1.848e-3)	4.912e-2$^+$ (1.667e-2)	9.861e-1$^+$ (9.575e-2)	***6.226e-3***$^+$ (7.053e-4)	***3.119e-2***$^+$ (9.776e-3)	***9.629e-1***$^+$ (1.545e-1)
UF8	1.313e-1$^+$ (3.384e-2)	2.669e-1$^+$ (8.397e-2)	1.328$^+$ (1.595e-1)	**1.199e-1** (3.828e-2)	**2.517e-1** (9.026e-2)	***1.234*** (1.516e-1)	1.562e-1$^+$ (6.280e-2)	3.673e-1$^+$ (1.860e-1)	1.939$^+$ (4.311e-1)	2.916e-1$^+$ (6.221e-2)	2.986e-1$^+$ (1.444e-1)	2.175$^+$ (2.827e-1)	***1.290e-1***$^+$ (4.725e-2)	***2.837e-1***$^+$ (1.155e-1)	**1.223** (2.165e-1)
UF9	**1.811e-1** (6.077e-2)	**3.574e-1** (1.071e-1)	**2.023** (3.626e-1)	2.106e-1$^+$ (4.425e-2)	4.084e-1$^+$ (7.544e-2)	2.375$^+$ (2.898e-1)	2.458e-1$^+$ (5.581e-2)	4.207e-1$^+$ (9.592e-2)	4.159$^+$ (1.268)	2.622e-1$^+$ (7.202e-2)	4.010e-1$^+$ (9.595e-2)	2.944$^+$ (3.770e-1)	***1.859e-1***$^+$ (6.342e-2)	***3.622e-1***$^+$ (1.137e-1)	***2.109***$^+$ (2.908e-1)
UF10	**4.266e-1** (8.360e-2)	**7.879e-1** (8.543e-2)	**2.176e+1** (5.837)	4.704e-1$^+$ (5.154e-2)	8.231e-1$^+$ (8.717e-2)	2.394e+1$^+$ (5.595)	7.964e-1$^+$ (1.051e-1)	1.019$^+$ (8.043e-2)	3.114e+1$^+$ (6.332)	1.171$^+$ (1.066e-1)	1.207$^+$ (5.860e-2)	2.816e+1$^+$ (7.417)	***4.384e-1***$^+$ (6.425e-2)	***7.858e-1***$^+$ (7.369e-2)	***2.253e+1***$^+$ (6.374)
UF11	**3.096e-1** (2.180e-2)	**4.278e-1** (4.426e-2)	**1.428** (7.914e-2)	4.982e-1$^+$ (4.893e-2)	5.386e-1$^+$ (1.454e-2)	1.891$^+$ (1.346e-1)	5.612e-1$^+$ (3.956e-2)	5.664e-1$^+$ (2.971e-2)	2.355$^+$ (8.719e-1)	4.027e-1$^+$ (3.806e-2)	5.328e-1$^+$ (2.458e-2)	1.638$^+$ (1.574e-1)	***3.146e-1***$^+$ (2.430e-2)	***5.239e-1***$^+$ (6.372e-2)	***1.446***$^+$ (7.464e-2)
UF12	**1.663e+2** (3.643e+1)	**1.667e+2** (3.621e+1)	**4.293e+2** (8.719e+1)	2.579e+2$^+$ (6.048e+1)	2.585e+2$^+$ (6.048e+1)	1.461e+3$^+$ (1.340e+2)	5.620e+2$^+$ (1.794e+2)	1.036e+3$^+$ (1.639e+2)	9.382e+2$^+$ (2.215e+3)	4.151e+3$^+$ (2.437e+2)	8.743e+2$^+$ (1.852e+2)	1.681e+2$^+$ (9.642e+2)	***1.873e+3***$^+$ (4.250e+1)	***1.676e+2***$^+$ (4.129e+1)	***4.532e+2***$^+$ (1.028e+2)
UF13	2.687$^+$ (1.531e-4)	5.829$^+$ (1.906e-4)	5.830e+1$^+$ (1.891e-3)	2.692$^+$ (7.464e-3)	5.845$^+$ (2.921e-3)	5.946e+1$^+$ (5.090e-2)	**2.631** (4.120e-2)	**5.809** (1.863e-2)	**5.627e+1** (4.188e-1)	***2.674***$^+$ (5.154e-3)	***5.827***$^+$ (2.106e-3)	***5.690e+1***$^+$ (7.376e-1)	2.701$^+$ (4.118e-2)	5.857$^+$ (3.635e-2)	5.716e+1$^+$ (1.602e-2)

TABLE IV

STATISTICS OF PERFORMANCE COMPARISONS BETWEEN OUR PROPOSED ALGORITHM AND OTHER COMPARED MOEAS. BASED ON THE WILCOXON RANK SUM TEST AT A 5% SIGNIFICANCE LEVEL, "+", "≈" AND "-" RESPECTIVELY IS THE NUMBER OF MOEA/D-2TCHMFI IS BETTER THAN, SIMILAR TO, AND WORSE THAN OTHER COMPARED ALGORITHM.

MOEA/D-2TCHMFI VS.	T test	MOEA/D-TCH	NSGA-III	SMS-EMOA	MOEA/D-MTCH
IGD	+	22	20	17	20
	≈	0	0	0	1
	-	1	3	6	2
$I_{\varepsilon+}$	+	22	20	17	20
	≈	0	0	0	1
	-	1	3	6	2
R_2^{2tch}	+	22	19	17	20
	≈	0	0	0	0
	-	1	4	6	3

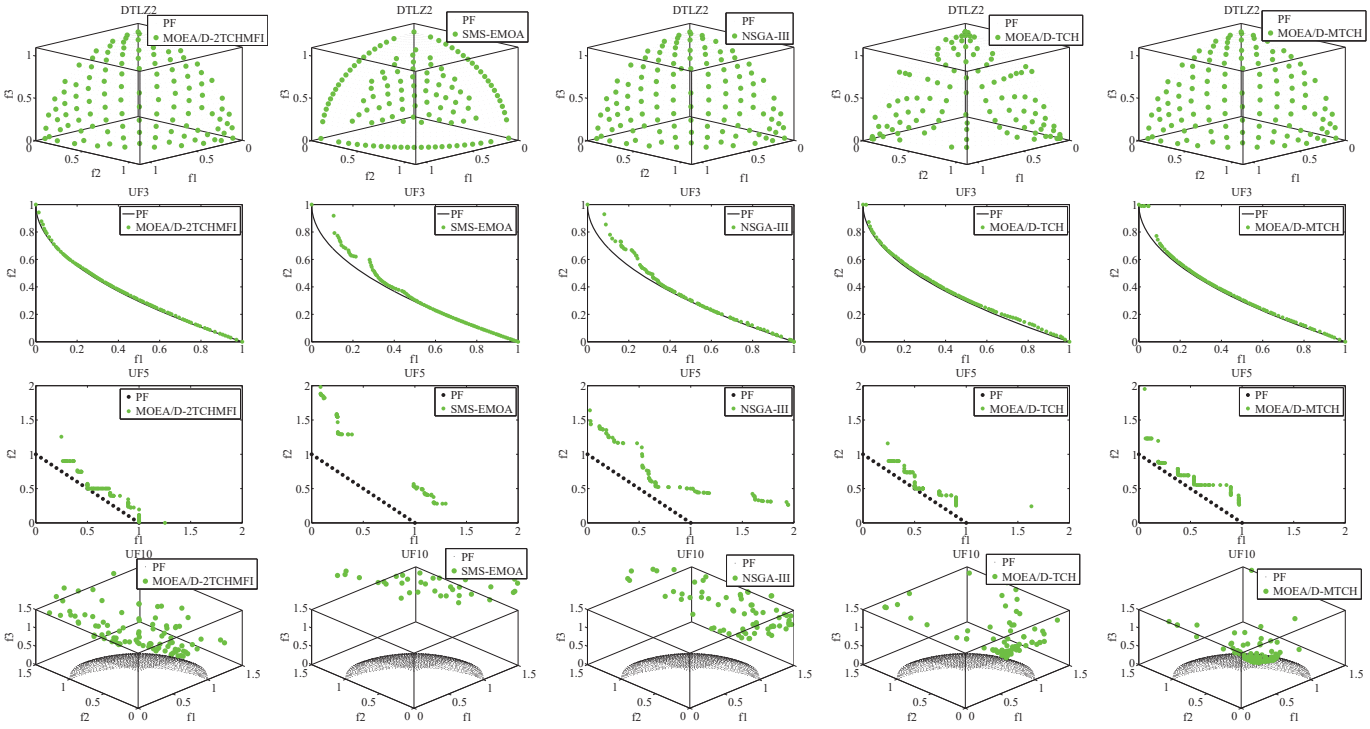

Fig. 11. The solution set with the median IGD values obtained by the compared algorithms.

RFC problem is defined as follows:

$$\begin{cases} \min \mathbf{F}(\mathbf{Q}) = \left(\max\limits_{1\le t\le T}(Z_t), \quad \max\limits_{1\le t\le T}(Q_t) \right) \\ \text{subject to}: t = 1, \ldots, T \\ \qquad Z_{min} \le Z_t \le Z_{max} \\ \qquad 0 \le Q_t \le Q_{max} \\ \qquad V_t = V_{t-1} + I_t - Q_t \\ \qquad Z_t = \Psi(V_t) \end{cases} \tag{21}$$

where Q_t, Z_t, V_t, and I_t indicate the discharge volume, the upstream water level, the reservoir storage, and the inflow volume in the t-th scheduling time interval, respectively. Q_{max} is the maximum discharge volume overall all scheduling periods. Z_{max} and Z_{min} are the upper and lower bounds of the upstream water level in the t-th scheduling interval, respectively. The reservoir storage of the t-th scheduling period V_t can be calculated by the water balance equation $V_t = V_{t-1} + I_t - Q_t$. The upstream water level of the t-th scheduling period Z_t can be obtained based on a problem-dependent function $\Psi(\cdot)$ taking the reservoir storage V_t as input. The problem is to find an optimal series of discharge volumes $\mathbf{Q} = (Q_1, \ldots, Q_T)$ in T scheduling periods such that the maximum discharge volume and the highest upstream water level are minimized.

Two representative real-world RFC problems, namely Ankang20000712 and Ankang20100715, of the Ankang reservoir in Shanxi province of China, are considered in this experimental study. Fig. 13 (a) describes a schematic diagram of the Ankang reservoir where Z_{max} and Z_{min} are set to 330m and 300m, respectively. The initial water level is set to 317m. The flood stage is set to 325m considering the security of reservoir. The maximum discharge volume Q_{max} is 37,474 m^3/s. Figs. 13 (b) and (c) illustrate the reservoir inflow volume of two floods happened on July 12, 2000 and July 15, 2010, respectively. Each flood has one flow crest. Fig. 13 (d) reflects the function $\Psi(\cdot)$ of the reservoir storage to the water level of the Ankang reservoir.

Table VII reports the mean and standard deviations of the

This article has been accepted for publication in a future issue of this journal, but has not been fully edited. Content may change prior to final publication. Citation information: DOI 10.1109/TEVC.2017.2704118, IEEE Transactions on Evolutionary Computation

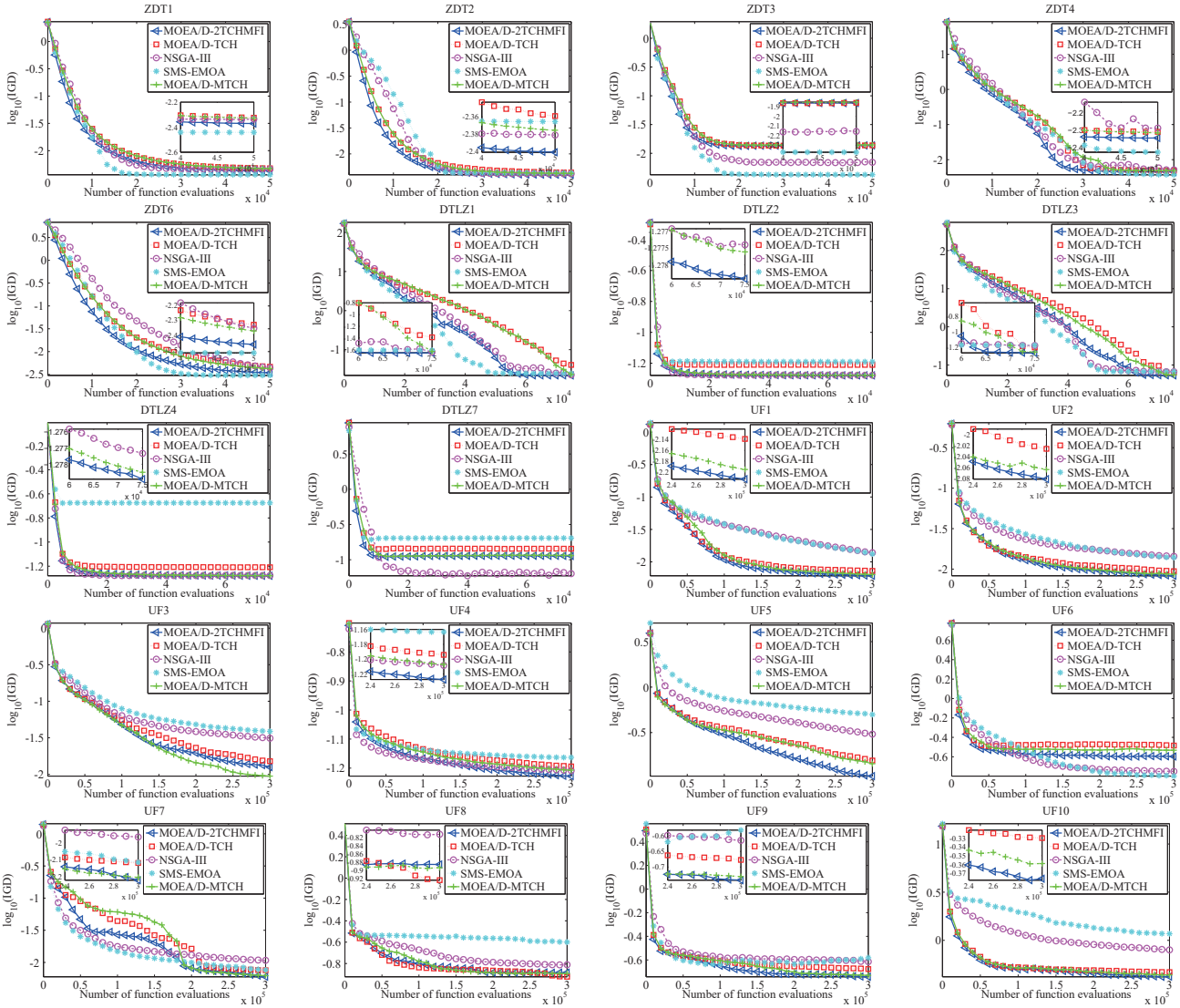

Fig. 12. Evolution of the mean of IGD-metric values on the test problems for five compared algorithms.

IGD, $I_{\epsilon+}$, and R_2^{2tch} metric values obtained by the compared algorithms on the two multi-objective RFC problems of Ankang reservoir. It shows that the final solutions obtained by MOEA/D-2TCHMFI are better than other compared algorithms in terms of the three metrics.

Fig. 14, taking IGD metric for example, illustrates the non-dominated solutions with the median IGD values obtained by four compared algorithms on the two investigated study cases. MOEA/D-2TCHMFI is shown to perform better than other compared algorithms in terms of both uniformity and convergence.

VIII. Conclusion

Tchebycheff decomposition is one of the most widely used decomposition methods. However, the geometric property of its subproblem objective functions has not been studied. This paper proposes a Tchebycheff decomposition with l_p-norm constraint on direction vectors (p-Tch) in which the subproblem objective functions have intuitive geometric property. Especially, the 2-Tch is taken as the representative to theoretically illustrate its advantage. A new unary R_2 indicator based on 2-Tch, i.e., R_2^{2tch}, is also introduced to approximate the hyper-volume metric and justify the efficiency of the proposed decomposition approach. The 2-Tch and a new population update strategy are integrated into MOEA/D to solve MOPs. Experimental results on both benchmark and real-world MOPs show that the proposed 2-Tch together with the new population update strategy can significantly improve the performance of MOEA/D. The resultant algorithm is capable of obtaining superior or comparable performance to the other state-of-the-art multi-objective evolutionary algorithms.

This work is expected to provide more insights into the Tchebycheff decomposition and a few interesting topics are still opened in the future work, e.g., 1) How to configure p is still an open question and the effects on other forms of $c(\mathbf{w})$ are worth studying. 2) The parent population is currently updated with only one offspring solution every time in the proposed population update strategy. However, it could be more beneficial to update the parent population with the whole offspring population. 3) How to use the R_2^{2tch}-metric to select a subset of non-dominated solutions

TABLE V

MEAN AND STANDARD DEVIATION OF IGD, AND R_2^{2tch} METRIC VALUES ON MOPS. THE VALUE WITHIN PARENTHESES IS THE DEVIATION OF METRIC. THE BEST MEAN VALUE IS HIGHLIGHTED WITH BOLD. BASED ON WILCOXON'S RANK SUM TEST AT 5% SIGNIFICANCE LEVEL, "+" IS THE PERFORMANCE OF BEST ALGORITHM ARE STATISTICALLY BETTER THAN OTHER COMPARED ALGORITHM. NO RESULT OF $I_{\epsilon+}$ METRIC VALUES ON THESE MOPS IS PROVIDED DUE TO SPACE LIMITATION.

Metric	MOEA/D-2TCHMFI		MOEA/D-TCH		MOEA/D-TCHMFI		MOEA/D-2TCH		MOEA/D-MTCHMFI		MOEA/D-MTCH	
	IGD	R_2^{2tch}	IGD	R_2^{2tch}	IGD	R_2^{2tch}	IGD	R_2^{2tch}	IGD	R_2^{2tch}	IGD	R_2^{2tch}
ZDT1	**4.616e-3** (2.373e-5)	**6.793e-1** (3.183e-3)	4.741e-3$^+$ (7.399e-5)	6.871e-1$^+$ (6.437e-3)	4.661e-3$^+$ (2.495e-5)	6.805e-1$^+$ (3.257e-3)	4.702e-3$^+$ (3.239e-5)	6.818e-1$^+$ (3.282e-3)	4.660e-3$^+$ (2.432e-5)	7.017e-1$^+$ (1.768e-4)	4.709e-3$^+$ (3.849e-5)	6.829e-1$^+$ (4.406e-3)
ZDT2	**4.155e-3** (1.020e-5)	**9.332e-1** (4.439e-3)	4.373e-3$^+$ (5.927e-5)	9.615e-1$^+$ (8.909e-3)	4.296e-3$^+$ (3.133e-5)	9.545e-1$^+$ (9.289e-3)	4.205e-3$^+$ (2.240e-5)	9.468e-1$^+$ (4.254e-3)	4.184e-3$^+$ (1.617e-5)	9.339e-1$^+$ (4.590e-4)	4.209e-3$^+$ (1.992e-5)	9.512e-1$^+$ (6.375e-3)
ZDT3	**1.371e-2** (9.388e-5)	**1.186** (3.077e-4)	1.376e-2$^+$ (2.564e-4)	1.189$^+$ (3.028e-3)	1.372e-2$^+$ (1.264e-4)	1.188$^+$ (4.799e-4)	1.400e-2$^+$ (6.192e-5)	1.187$^+$ (1.421e-3)	1.400e-2$^+$ (6.342e-5)	1.186$^+$ (1.921e-4)	1.374e-2$^+$ (9.908e-5)	1.187$^+$ (2.052e-3)
ZDT4	4.793e-3$^+$ (1.447e-4)	6.844e-1$^+$ (1.226e-2)	4.884e-3$^+$ (1.297e-4)	6.943e-1$^+$ (1.397e-2)	4.800e-3$^+$ (1.386e-4)	6.885e-1$^+$ (1.309e-2)	4.831e-3$^+$ (1.308e-4)	6.856e-1$^+$ (1.104e-2)	**4.771e-3** (1.684e-4)	**6.833e-1** (1.358e-2)	4.815e-3$^+$ (1.386e-4)	6.868e-1$^+$ (1.228e-2)
ZDT6	**3.724e-3** (1.084e-4)	**7.387e-1** (6.449e-3)	4.657e-3$^+$ (3.741e-4)	7.713e-1$^+$ (1.667e-2)	3.910e-3$^+$ (1.531e-4)	7.458e-1$^+$ (9.280e-3)	4.224e-3$^+$ (2.560e-4)	7.554e-1$^+$ (1.366e-2)	3.732e-3$^+$ (9.137e-5)	7.394e-1$^+$ (9.172e-4)	4.232e-3$^+$ (2.263e-4)	7.577e-1$^+$ (1.167e-2)
DTLZ1	2.207e-2$^+$ (3.380e-3)	4.132e-1$^+$ (1.261e-2)	4.225e-2$^+$ (6.952e-2)	4.847e-1$^+$ (2.784e-2)	3.250e-2$^+$ (5.019e-2)	4.509e-1$^+$ (3.035e-1)	2.215e-2$^+$ (1.182e-4)	4.496e-1$^+$ 7(2.787e-2)	**2.180e-2** (2.948e-4)	**4.024e-1** (1.287e-2)	2.336e-2$^+$ (4.196e-2)	4.793e-1$^+$ (1.669e-1)
DTLZ2	5.267e-2$^+$ (1.434e-4)	1.055$^+$ (2.187e-2)	6.165e-2$^+$ (3.839e-4)	1.106$^+$ (2.080e-2)	6.163e-2$^+$ (2.670e-4)	1.168$^+$ (1.021e-1)	5.269e-2$^+$ (1.361e-4)	1.057$^+$ (2.864e-2)	**5.265e-2** (1.257e-4)	**1.037** (6.026e-4)	5.278e-2$^+$ (1.638e-4)	1.061$^+$ (2.995e-2)
DTLZ3	**5.333e-2** (5.819e-4)	**1.158** (6.767e-2)	6.284e-2$^+$ (4.070e-3)	1.256$^+$ (1.486e-1)	6.169e-2$^+$ (4.797e-4)	1.224$^+$ (1.016e-1)	5.402e-2$^+$ (9.267e-4)	1.283$^+$ (1.722e-1)	5.345e-2$^+$ (8.712e-3)	1.057$^+$ (1.983e-2)	5.430e-2$^+$ (1.624e-3)	1.343$^+$ (2.354e-1)
DTLZ4	**5.265e-2** (1.467e-4)	**1.034** (3.466e-3)	6.194e-2$^+$ (3.736e-4)	1.071$^+$ (1.278e-2)	6.181e-2$^+$ (2.935e-4)	1.133$^+$ (7.324e-2)	5.273e-2$^+$ (1.360e-4)	1.042$^+$ (2.277e-3)	5.269e-2$^+$ (1.737e-4)	1.037$^+$ (3.787e-4)	5.266e-2$^+$ (1.653e-4)	1.039$^+$ (1.421e-3)
DTLZ7	**1.130e-1** (3.171e-3)	**2.416** (4.842e-2)	1.433e-1$^+$ (1.255e-3)	2.437$^+$ (6.814e-3)	1.432e-1$^+$ (9.688e-4)	2.435$^+$ (1.186e-3)	1.137e-1$^+$ (3.286e-3)	2.425$^+$ (4.802e-2)	1.136e-1$^+$ (3.655e-3)	2.436$^+$ (6.555e-2)	1.137e-1$^+$ (3.340e-3)	2.444$^+$ (7.315e-2)
UF1	**6.113e-3** (3.431e-4)	**7.090e-1** (1.192e-2)	7.265e-3$^+$ (1.555e-3)	7.105e-1$^+$ (1.349e-2)	6.879e-3$^+$ (4.649e-4)	7.102e-1$^+$ (1.369e-2)	6.177e-3$^+$ (2.960e-4)	7.107e-1$^+$ (1.009e-2)	6.270e-3$^+$ (5.214e-4)	7.271e-1$^+$ (1.425e-2)	6.171e-3$^+$ (3.937e-4)	7.099e-1$^+$ (1.027e-2)
UF2	**8.281e-3** (9.953e-4)	**7.688e-1** (1.778e-1)	9.422e-3$^+$ (7.101e-4)	8.224e-1$^+$ (1.297e-1)	9.025e-3$^+$ (1.006e-3)	8.299e-1$^+$ (1.350e-1)	8.806e-3$^+$ (1.149e-3)	8.391e-1$^+$ (1.709e-1)	8.832e-3$^+$ (1.480e-3)	8.187e-1$^+$ (1.218e-1)	8.425e-3$^+$ (1.639e-3)	7.915e-1$^+$ (1.679e-1)
UF3	1.256e-2$^+$ (9.497e-3)	8.305e-1$^+$ (3.983e-1)	1.316e-2$^+$ (9.922e-3)	8.338e-1$^+$ (4.426e-1)	1.496e-2$^+$ (9.922e-3)	8.912e-1$^+$ (5.005e-1)	1.018e-2$^+$ (8.810e-3)	8.273e-1$^+$ (4.275e-1)	1.288e-2$^+$ (1.341e-2)	8.711e-1$^+$ (4.891e-1)	**9.478e-3** (5.180e-3)	**8.239e-1** (4.207e-1)
UF4	5.928e-2$^+$ (3.698e-3)	2.143$^+$ (1.455e-1)	6.411e-2$^+$ (4.917e-3)	2.273$^+$ (3.410e-1)	6.193e-2$^+$ (5.406e-3)	2.134$^+$ (2.138e-1)	6.255e-2$^+$ (4.896e-3)	2.158$^+$ (2.900e-1)	**5.827e-2** (3.787e-3)	**1.200** (4.952e-2)	6.252e-2$^+$ (5.020e-3)	2.188$^+$ (2.045e-1)
UF5	1.058e-1$^+$ (2.468e-2)	7.010$^+$ (6.016)	1.572e-1$^+$ (7.468e-2)	1.469e+1$^+$ (1.165e+1)	1.220e-1$^+$ (6.016e-2)	1.061e+1$^+$ (8.471)	1.540e-1$^+$ (7.177e-2)	1.503e+1$^+$ (1.371e+1)	**9.162e-2** (1.829e-2)	**6.516** (6.162)	1.473e-1$^+$ (7.445e-2)	1.346e+1$^+$ (1.017e+1)
UF6	**2.601e-1** (1.584e-1)	**3.084** (2.216)	3.387e-1$^+$ (2.174e-1)	4.283$^+$ (2.306)	2.970e-1$^+$ (1.798e-1)	3.753$^+$ (2.216)	2.924e-1$^+$ (1.331e-1)	3.662$^+$ (3.160)	3.368e-1$^+$ (1.993e-1)	1.649e+2$^+$ (9.392e+1)	2.982e-1$^+$ (1.788e-1)	3.741$^+$ (1.953)
UF7	6.192e-3$^+$ (2.454e-3)	9.233e-1$^+$ (1.260e-1)	7.571e-3$^+$ (2.164e-3)	9.892e-1$^+$ (2.070e-1)	6.894e-3$^+$ (1.291e-3)	9.434e-1$^+$ (1.124e-1)	6.274e-3$^+$ (8.321e-4)	9.337e-1$^+$ (1.218e-1)	**5.841e-3** (3.303e-4)	**8.525e-1** (3.323e-2)	6.226e-3$^+$ (7.053e-4)	9.629e-1$^+$ (1.545e-1)
UF8	1.313e-1$^+$ (3.384e-2)	1.328$^+$ (1.595e-1)	1.199e-1$^+$ (3.828e-2)	1.234$^+$ (1.516e-1)	1.414e-1$^+$ (7.597e-2)	1.361$^+$ (3.282e-1)	**1.187e-1** (2.541e-2)	**1.157** (2.119e-2)	1.429e-1$^+$ (6.394e-2)	1.268$^+$ (2.968e-1)	1.290e-1$^+$ (4.725e-2)	1.223$^+$ (2.165e-1)
UF9	1.811e-1$^+$ (6.077e-2)	**2.023** (3.626e-1)	2.106e-1$^+$ (4.425e-2)	2.375$^+$ (2.898e-1)	1.809e-1$^+$ (5.879e-2)	2.142$^+$ (3.908e-1)	**1.711e-1** (6.513e-2)	2.051 (2.999e-1)	1.959e-1$^+$ (5.541e-2)	2.096$^+$ (3.019e-1)	1.859e-1$^+$ (6.342e-2)	2.109$^+$ (2.908e-1)
UF10	4.266e-1$^+$ (8.360e-2)	2.176e+1$^+$ (5.837)	4.704e-1$^+$ (5.154e-2)	2.394e+1$^+$ (5.595)	4.499e-1$^+$ (4.331e-2)	2.285e+1$^+$ (8.076)	4.330e-1$^+$ (6.002e-2)	2.207e+1$^+$ (6.782)	**4.106e-1** (9.360e-2)	**1.927e+1** (1.040e+1)	4.384e-1$^+$ (6.425e-2)	2.253e+1$^+$ (6.374)

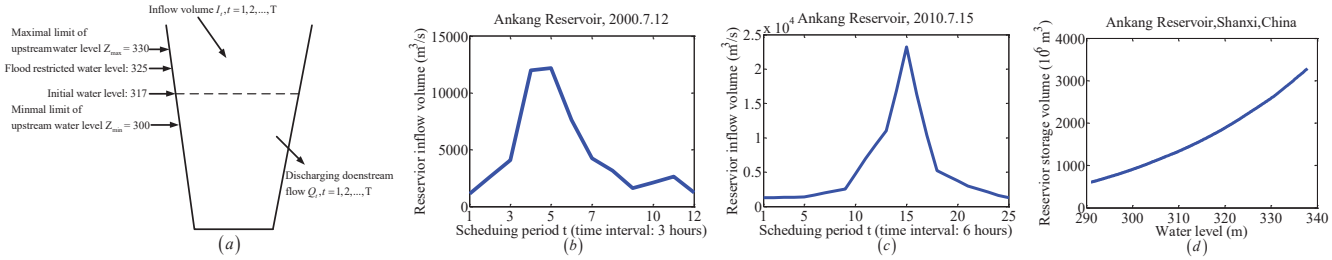

Fig. 13. (a) A schematic diagram of Ankang reservoir. (b)-(c) The inflow volume information of the Ankang reservoir on July 12, 2000 and July 15, 2010. (d) The water level to volume curve of the Ankang reservoir.

TABLE VII

STATISTIC IGD, $I_{\epsilon+}$, AND R_2^{2tch} METRIC VALUES OF THE SOLUTIONS FOUNDED BY THREE ALGORITHMS ON THE TWO RESERVOIR FLOOD CONTROL PROBLEMS ANKANG20000712 AND ANKANG20100715, THE NUMBERS IN PARENTHESES PRESENT THE STANDARD DEVIATION.

Metric	MOEA/D-2TCHMFI			MOEA/D-TCH			NSGA-III			MOEA/D-MTCH		
	IGD	$I_{\epsilon+}$	R_2^{2tch}	IGD	$I_{\epsilon+}$	R_2^{2tch}	IGD	$I_{\epsilon+}$	R_2^{2tch}	IGD	$I_{\epsilon+}$	R_2^{2tch}
Ankang20000712	**1.3327e+4** (1.5727e+2)	**1.3983e+2** (1.9250)	**3.9351e+4** (6.30002)	1.3445e+4$^+$ (3.9886e+2)	1.4583e+2$^+$ (2.5296)	4.0513e+4$^+$ (7.6494)	1.3395e+4$^+$ (1.6232e+2)	1.4133e+2$^+$ (2.2296)	3.9779e+4$^+$ (1.0428e+2)	1.3401e+4$^+$ (1.6574e+2)	1.4386e+2$^+$ (2.2486)	4.0310e+4$^+$ (8.9839)
Ankang20100715	**1.3202e+4** (1.9717e+1)	**3.6252e+2** (4.8773)	**5.0751e+4** (2.4431e+2)	1.3325e+4$^+$ (2.5793e+1)	3.769e+2$^+$ (8.3598)	5.2479e+4$^+$ (3.8964e+2)	1.3208e+4$^+$ (2.2106e+1)	3.6318e+2$^+$ (6.1457)	5.1801e+4$^+$ (2.8815+2)	1.3205e+4$^+$ (2.3948e+1)	3.7381+2$^+$ (5.4629)	5.2410e+4$^+$ (2.6876e+2)

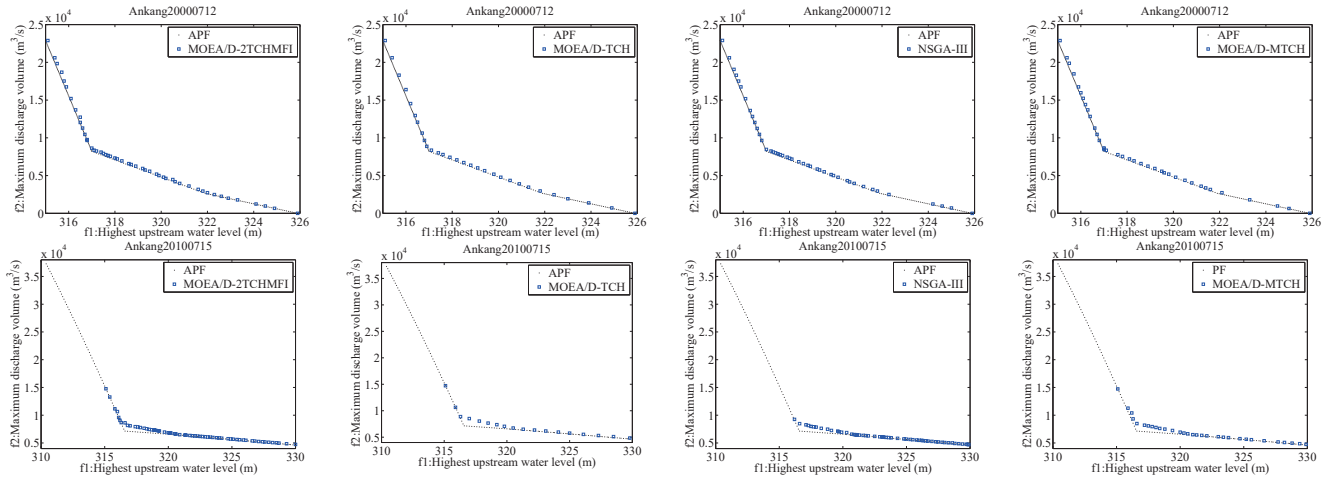

Fig. 14. The solution set with the median IGD values obtained by the compared algorithms on two RFC problems Ankang20000712 and Ankang20100715. No result of SMS-EMOA on these two problems is provided due to some incompatibilities of the algorithm source code to the RFC problems.

deserves more investigation. 4) Introducing local search [48–54] is an interesting direction to improve the efficiency of the algorithm. 5) Investigating different neighbor structures [55] of the subproblems is also an interesting topic.

The source code and the supplementary material are available at http://csse.szu.edu.cn/staff/zhuzx/MOEAD-2TCHMFI.html.

REFERENCES

[1] K. Deb, *Multi-Objective Optimization Using Evolutionary Algorithms*. Wiley, 2001.

[2] C. Coello, G. Lamont, and D. Veldhuizen, *Evolutionary Algorithms for Solving Multi-Objective Problems*. Springer, 2007.

[3] Q. Zhang and H. Li, "MOEA/D: A multi-objective evolutionary algorithm based on decomposition," *IEEE Transactions on Evolutionary Computation*, vol. 11, no. 6, pp. 712–731, 2007.

[4] H. Li and D. Landa-Silva, "An adaptive evolutionary multi-objective approach based on simulated annealing," *Evolutionary Computation*, vol. 19, no. 4, pp. 561–595, 2011.

[5] I. Giagkiozis, R. Purshouse, and P. Fleming, "Generalized decomposition and cross entropy methods for many-objective optimization," University of Sheffield, Tech. Rep. 1029, 2012.

[6] ——, "Generalized decomposition and cross entropy methods for many-objective optimization," *Information Sciences*, vol. 282, pp. 363–387, 2014.

[7] ——, "Generalized decomposition," in *International Conference on Evolutionary Multi-Criterion Optimization (EMO)*, 2013, pp. 428–442.

[8] Y. Qi, X. Ma, F. Liu, L. Jiao, J. Sun, and J. Wu, "MOEA/D with adaptive weight adjustment," *Evolutionary Computation*, vol. 22, no. 2, pp. 231–264, 2014.

[9] K. Deb and H. Jain, "An evolutionary many-objective optimization algorithm using reference-point based non-dominated sorting approach, Part I: Solving problems with box constraints," *IEEE Transactions on Evolutionary Computation*, vol. 18, no. 4, pp. 577–601, 2014.

[10] ——, "An improved NSGA-II procedure for many-objective optimization, Part I: Solving problems with box constraints," KanGAL, Tech. Rep. 2012009, 2012.

[11] Q. Zhang, H. Li, D. Maringer, and E. Tsang, "MOEA/D with NBI-style Tchebycheff approach for portfolio management," in *Proceedings of the 2010 IEEE Congress on Evolutionary Computation*, 2010, pp. 1–8.

[12] H. Ishibuchi, Y. Sakane, N. Tsukamoto, and Y. Nojima, "Adaptation of scalarizing functions in MOEA/D: An adaptive scalarizing function-based multiobjective evolutionary algorithm," in *Proceedings of the 2009 International Conference on Evolutionary Multi-Criterion Optimization*, 2009, pp. 438–452.

[13] I. Giagkiozis, R. Purshouse, and P. Fleming, "An overview of population-based algorithms for multi-objective optimization," *International Journal of Systems Science*, vol. 46, no. 9, pp. 1572–1599, 2015.

[14] Z. Zhu, J. Xiao, J.-Q. Li, F. Wang, and Q. Zhang, "Global path planning of wheeled robots using multi-objective memetic algorithms," *Integrated Computer-Aided Engineering*, vol. 22, no. 4, pp. 387–404, 2015.

[15] M. Hansen and A. Jaszkiewicz, "Evaluating the quality of approximations of the nondominated set," Technical University of Denmark, IMM Technical Report IMM-REP-1998-7, 1998.

[16] Q. Zhang, W. Liu, and H. Li, "The performance of a new version of MOEA/D on CEC09 unconstrained MOP test instances," in *Proceedings of the 2009 IEEE Congress on Evolutionary Computation*, 2009, pp. 203–208.

[17] H. Li and Q. Zhang, "Multiobjective optimization problems with complicated Pareto sets, MOEA/D and NSGA-II," *IEEE Transaction on Evolutionary Computation*, vol. 12, no. 2, pp. 284–302, 2009.

[18] S. Zhao, P. Suganthan, and Q. Zhang, "Decomposition-based multiobjective evolutionary algorithm with an ensemble of neighborhood sizes," *IEEE Transactions on Evolutionary Computation*, vol. 16, no. 3, pp. 442–446, 2012.

[19] Z. Wang, Q. Zhang, A. Zhou, M. Gong, and L. Jiao, "Adaptive replacement strategies for MOEA/D," *IEEE Transactions on Cybernetics*, vol. 46, no. 2, pp. 474–486, 2016.

[20] K. Miettinen, *Nonlinear Multiobjective Optimization*. Kluwer Academic Publishers, 1999.

[21] S. Boyd and L. Vandenberghe, *Convex Optimization*. Cambridge University Press, 2004.

[22] F. Gu, H. Liu, and K. Tan, "A multiobjective evolutionary algorithm using dynamic weight design method," *International Journal of Innovative Computing*, vol. 8, no. 5, pp. 3677–3688, 2012.

[23] X. Ma, F. Liu, Y. Qi, L. Li, L. Jiao, X. Deng, X. Wang, B. Dong, Z. Hou, Y. Zhang, and J. Wu, "MOEA/D with biased weight adjustment inspired by user preference and its application on multi-objective reservoir flood control problem," *Soft Computing*, vol. 20, no. 12, pp. 4999–5023, 2016.

[24] Y. Yuan, X. Hua, and B. Wang, "Evolutionary many-objective optimization using ensemble fitness ranking," in *Proceedings of the 2014 Annual Conference on Genetic and Evolutionary Computation*, 2014, pp. 669–676.

[25] H. Liu, F. Gu, and Q. Zhang, "Decomposition of a multiobjective optimization problem into a number of simple mul-

tiobjective subproblems," *IEEE Transaction on Evolutionary Computation*, vol. 18, no. 3, pp. 450–455, 2014.
[26] K. Li, S. Kwong, and K. Deb, "A dual population paradigm for evolutionary multiobjective optimization," *Information Sciences*, vol. 309, pp. 50–72, 2015.
[27] E. Zitzler, K. Deb, and L. Thiele, "Comparison of multiobjective evolutionary algorithms: Empirical results," *Evolutionary Computation*, vol. 8, no. 2, pp. 173–195, 2000.
[28] K. Deb, L. Thiele, M. Laumanns, and E. Zitzler, "Scalable multi-objective optimization test problems," *Proceedings of the 2002 IEEE Congress on Evolutionary Computation*, pp. 825–830, 2002.
[29] K. Deb and H. Beyer, "Self-adaptive genetic algorithms with simulated binary crossover," *Evolutionary Computation*, vol. 9, no. 2, pp. 197–221, 2001.
[30] K. Li, Q. Zhang, S. Kwong, M. Li, and R. Wang, "Stable matching based selection in evolutionary multiobjective optimization," *IEEE Transactions on Evolutionary Computation*, vol. 18, no. 6, pp. 909–923, 2014.
[31] K. Li, S. Kwong, Q. Zhang, and K. Deb, "Interrelationship-based selection for decomposition multiobjective optimization," *IEEE Transactions on Cybernetics*, vol. 45, no. 10, pp. 2076–2088, 2015.
[32] A. Zhou and Q. Zhang, "Are all the subproblems equally important? resource allocation in decomposition based multiobjective evolutionary algorithms," *IEEE Transaction on Evolutionary Computation*, vol. 20, no. 1, pp. 52–64, 2016.
[33] R. Gomez and C. Coello, "Improved metaheuristic based on the R2 indicator for many-objective optimization," in *Proceedings of the 2015 Genetic and Evolutionary Computation Conference*, 2015, pp. 679–686.
[34] ——, "MOMBI: A new metaheuristic for many-objective optimization based on the R2 indicator," in *Proceedings of the 2013 IEEE Congress on Evolutionary Computation*, 2013, pp. 2488–2495.
[35] H. Ishibuchi, N. Tsukamoto, S. Y., and Y. Nojima, "Hypervolume approximation using achievement scalarizing functions for evolutionary many-objective optimization," in *Proceedings of the 2009 IEEE Congress on Evolutionary Computation*, 2009, pp. 530–537.
[36] T. Wagner, H. Trautmann, and D. Brockhoff, "Preference articulation by means of the R2 indicator," in *Proceedings of the 2013 International Conference on Evolutionary Multi-Criterion Optimization*, 2013, pp. 81–95.
[37] D. Brockhoff, T. Wagner, and H. Trautmann, "On the properties of the R2 indicator," in *Proceedings of the 14th Annual Conference on Genetic and Evolutionary Computation*, 2012, pp. 465–472.
[38] D. Phan and J. Suzuki, "R2-IBEA: R2 indicator based evolutionary algorithm for multiobjective optimization," in *Proceedings of the 2013 IEEE Congress on Evolutionary Computation*, 2013, pp. 1836–1845.
[39] W. Dunham, *The Calculus Gallery: Masterpieces from Newton to Lebesgue*. Princeton University Press, 2004.
[40] E. Zitzler, L. Thiele, M. Laumanns, C. Fonseca, and V. Fonseca, "Performance assessment of multiobjective optimizers: An analysis and review," *IEEE Transactions on Evolutionary Computation*, vol. 7, no. 2, pp. 117–132, 2003.
[41] N. Beume, B. Naujoks, and M. Emmerich, "SMS-EMOA: Multiobjective selection based on dominated hypervolume," *European Journal of Operational Research*, vol. 181, no. 3, pp. 1653–1669, 2007.
[42] Q. Zhang, A. Zhou, S. Zhao, P. Suganthan, W. Liu, and S. Tiwari, "Multiobjective optimization test instances for the CEC 2009 special session and competition," University of Essex, Tech. Rep. CES-887, 2008.
[43] Y. Qi, F. Liu, M. Liu, M. Gong, and L. Jiao, "Multi-objective immune algorithm with Baldwinian learning," *Applied Soft Computing*, vol. 12, no. 8, pp. 2654–2674, 2012.
[44] Y. Qi, L. Bao, Y. Sun, J. Luo, and Q. Miao, "A memetic multi-objective immune algorithm for reservoir flood control operation," *Water Resources Management*, vol. 30, no. 9, pp. 2957–2977, 2016.
[45] K. Deb, A. Sinha, and S. Kukkonen, "Multi-objective test problems, linkages, and evolutionary methodologies," in *Proceedings of the 2006 Genetic and Evolutionary Computation Conference*, 2006, pp. 1141–1148.
[46] S. Huband, P. Hingston, L. Barone, and L. While, "A review of multiobjective test problems and a scalable test problem toolkit," *IEEE Transaction on Evolutionary Computation*, vol. 10, no. 5, pp. 477–506, 2006.
[47] X. Ma, F. Liu, Y. Qi, X. Wang, L. Li, L. Jiao, M. Yin, and M. Gong, "A multi-objective evolutionary algorithm based on decision variable analyses for multi-objective optimization problems with large scale variables," *IEEE Transactions on Evolutionary Computation*, vol. 20, no. 2, pp. 275–298, 2016.
[48] X. Ma, F. Liu, Y. Qi, L. Li, L. Jiao, M. Liu, and J. Wu, "MOEA/D with baldwinian learning inspired by the regularity property of continuous multiobjective problem," *Neurocomputing*, vol. 145, pp. 336–352, 2014.
[49] X. Ma, F. Liu, Y. Qi, M. Gong, M. Yin, L. Li, L. Jiao, and J. Wu, "MOEA/D with opposition-based learning for multiobjective optimization problem," *Neurocomputing*, vol. 146, pp. 48–64, 2014.
[50] X. Ma, Y. Qi, L. Li, F. Liu, L. Jiao, and J. Wu, "MOEA/D with uniform decomposition measurements for many-objective problems," *Soft Computing*, vol. 18, no. 12, pp. 2541–2564, 2014.
[51] Z. Zhu, Y.-S. Ong, and M. Dash, "Wrapper–filter feature selection algorithm using a memetic framework," *IEEE Transactions on Systems, Man, and Cybernetics, Part B: Cybernetics*, vol. 37, no. 1, pp. 70–76, 2007.
[52] Z. Zhu, J. Zhou, Z. Ji, and Y.-H. Shi, "DNA sequence compression using adaptive particle swarm optimization-based memetic algorithm," *IEEE Transactions on Evolutionary Computation*, vol. 15, no. 5, pp. 643–658, 2011.
[53] Z. Zhu, Y.-S. Ong, and J. M. Zurada, "Identification of full and partial class relevant genes," *IEEE/ACM Transactions on Computational Biology and Bioinformatics*, vol. 7, no. 2, pp. 263–277, 2010.
[54] Z. Zhu, J. Xiao, S. He, Z. Ji, and Y. Sun, "A multi-objective memetic algorithm based on locality-sensitive hashing for one-to-many-to-one dynamic pickup-and-delivery problem," *Information Sciences*, vol. 329, pp. 73–89, 2016.
[55] Y. Sun, L. Jiao, X. Deng, and R. Wang, "Dynamic network structured immune particle swarm optimisation with small-world topology," *International Journal of Bio-Inspired Computation*, 2017, in press.

Xiaoliang Ma received the B.S. degree in computing computer science and technology from Zhejiang Normal University, China in 2006, and the PH.D. degree at the school of computing of Xidian University, China in 2014. He is currently a postdoctor with the College of Computer Science and Software Engineering, Shenzhen University, China.

His research interests include evolutionary computation, multiobjective optimization, complex network, cooperative coevolution, bioinformatics.

Qingfu Zhang (M'01-SM'06-F'17) received the BSc degree in mathematics from Shanxi University, China in 1984, the MSc degree in applied mathematics and the PhD degree in information engineering from Xidian University, China, in 1991 and 1994, respectively.

He is a Professor at the Department of Computer Science, City University of Hong Kong, Hong Kong, and a Changjiang Visiting Chair Professor in Xidian University, China. His main research interests include evolutionary computation, optimization, neural networks, data analysis, and their applications. He is currently leading the Metaheuristic Optimization Research (MOP) Group in City University of Hong Kong.

Dr. Zhang is an Associate Editor of the IEEE Transactions on Evolutionary Computation and the IEEE Transactions on Cybernetics. He is also an Editorial Board Member of three other international journals. MOEA/D, a multiobjective optimization algorithmic framework, developed in his group, is one of the most widely used and researched multiobjective algorithms. He was awarded the 2010 IEEE Transactions on Evolutionary Computation Outstanding Paper Award. He is a 2016 Web of Science highly cited researcher in Computer Science.

Guangdong Tian received the B.S. degree in vehicle engineering from the Shandong University of Technology, Zibo, China, in 2007, and the M.S. and Ph.D. degrees in automobile application engineering from Jilin University, Changchun, China, in 2009 and 2012, respectively. He is currently an Associate Professor with the College of Transportation, Jilin University, Changchun, China.

His current research interests include remanufacturing and green manufacturing, green logistics and transportation, intelligent inspection and repair of automotive, decision-making, and intelligent optimization. He has published over 50 journal and conference proceedings papers in the above areas, including in the IEEE TRANSACTIONS ON AUTOMATION SCIENCE AND ENGINEERING, Computers and Chemical Engineering, and Computers and Industrial Engineering. Dr. Tian is listed in Marquis Whos Who in the World, 30th Edition, in 2013.

Junshan Yang received his B.S. degree from the School of Electronics and Information Engineering of Liaoning University of Technology, China, in 2004. He received his M.S. degree from the School of Physics and Telecommunication Engineering of South China Normal University, China, in 2008. He is currently a PhD student with the School of Engineering and Information, Shenzhen University, China.

His current research interests include evolutionary computation, bioinformatics, machine learning.

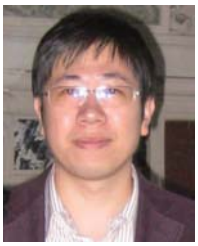

Zexuan Zhu received the B.S. degree in computer science and technology from Fudan University, China, in 2003 and the Ph.D. degree in computer engineering from Nanyang Technological University, Singapore, in 2008. He is currently a Professor with the College of Computer Science and Software Engineering, Shenzhen University, China.

His research interests include computational intelligence, machine learning, and bioinformatics. Dr. Zhu is an Associate Editor of IEEE Transactions on Evolutionary Computation and IEEE Transactions on Emerging Topics in Computational Intelligence, and serves as the Editorial Board Member of Memetic Computing Journal and Soft Computing Journal. He is also a Vice Chair of the IEEE Emergent Technologies Task Force on Memetic Computing.